Master's Theses   Master's Theses and Graduate Research

2003

Chiral separation by RP-HPLC

Huy Tu Nguyen
San Jose State University

CHIRAL SEPARATION BY RP-HPLC

A Thesis

Presented to

The Faculty of the Department of Chemistry

San Jose State University

In Partial Fulfillment

of the Requirements for the Degree

Master of Science

by

Huy Tu Nguyen

May 2003

UMI Number: 1415725

UMI®

UMI Microform 1415725
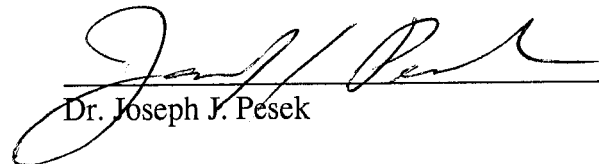
APPROVED FOR THE DEPARTMENT OF CHEMISTRY

Dr. Joseph J. Pesek

Dr. Roy K. Okuda

Dr. Roger H. Terrill

APPROVED FOR THE UNIVERSITY

ABSTRACT

CHIRAL SEPARATION BY RP-HPLC

by Huy Tu Nguyen

Initially, the chiral selector, 2-hydroxy-3-methacryloyloxypropyl-β-cyclodextrin, was further tested to examine if other solutes could be partitioned besides temazepam, oxazepam, and dansyl-DL-leucine. Another chiral selector, quinine, was chosen to compare with the substituted β-cyc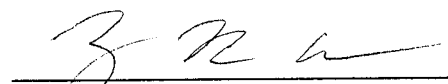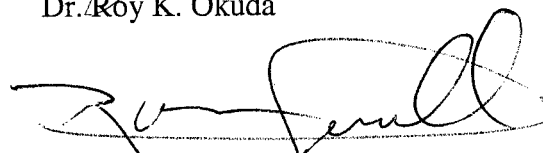lodextrin. Vydac silica hydride was synthesized by TES silanization. Quinine was attached to the silica hydride by hydrosilation. The products were analyzed by DRIFT spectroscopy, ^{13}C CP-MAS NMR spectroscopy, and elemental analysis.

Separation of optical isomers was achieved on both columns on multiple solutes such as clenbuterol, tropicamide, and novel Selenium compounds. The mechanism of separation for most of the solutes were Pirkle type interactions. The 2-hydroxy-3-methacryloyloxypropyl-β-cyclodextrin column achieved more separation than the quinine column probably due to the ability to form inclusion complexes besides other interactions. Solvent systems consisting of buffers at pH 2.0 and 7.0, respectively, decreased the ability of quinine to separate some enantiomers relative to methanol/water and acetonitrile/water.

Acknowledgements

First of all, I would like to thank my research advisor, Dr. Joseph J. Pesek, and Dr. Maria Matyska for allowing me to join their excellent research group. Also, I would like to express my gratitude to both professors for having great patience and providing guidance throughout my research project. None of this work would have been possible without their expert assistance with the various instrumentations. Additionally, I would like to thank my committee members, Dr. Roy K. Okuda and Dr. Roger H. Terrill, for taking their valuable time to review my thesis and giving me suggestions. Last of all, I would like to thank my family (Dad, Mom, and Brother) for their love, support, and guidance throughout my whole life.

Table of Contents

List of Figures

List of Tables

CHAPTER I

INTRODUCTION AND BACKGROUND

A. Chromatography

In various fields of science, such as analytical chemistry and biochemistry, chromatography is used as a technique to purify, identify, and quantify specific molecules from a mixture. The three components in chromatography are: stationary phase, mobile phase, and solute. The stationary phase, or adsorbant, is the solid medium in which the specific molecules of interest adhere. The mobile phase is the liquid (solvent), or gas, that flows over the stationary phase. The solute is the specific molecule of interest that one desires to isolate from a complex mixture. The solute is soluble in the mobile phase; if this was not the case, the solute could be separated by physical means, such as filtration. Figure 1 illustrates the three components in chromatography.

The fundamental principle of chromatography is that separation of solutes occurs because of different physical (e.g. size) or chemical properties (i.e., polarity, charge, unique affinity), which results in different retention times. Retention time is a parameter that indicates the amount of time a solute takes to elute from the column or how strong the solute adheres to the stationary phase. Hence, longer retention times represent stronger interactions between the solute and the stationary phase. Multiple types of chromatography exist – for example, thin-layer chromatography (TLC), gas chromatography (GC), and column chromatography. An example of column chromatography is high- performance liquid chromatography (HPLC),

Figure 1. Components in chromatography.

S = Solute molecules

◯ = Stationary phase
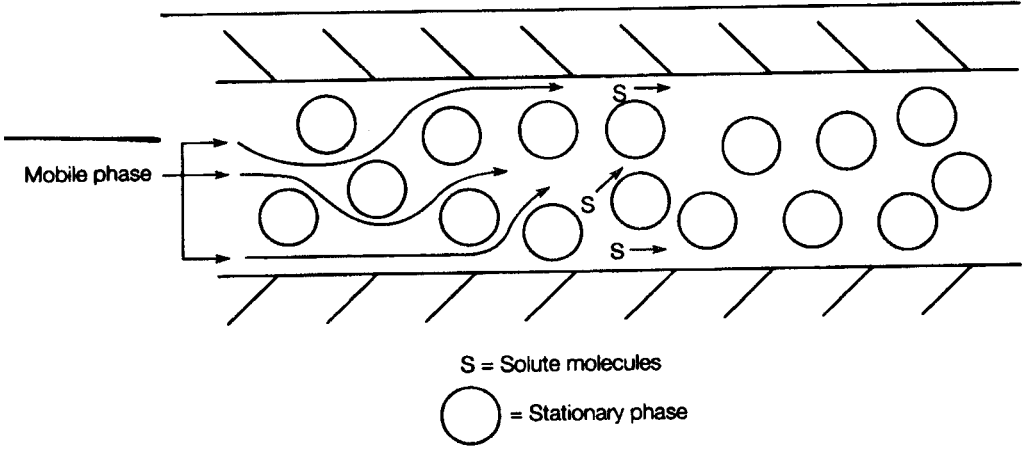
which was used in this research project.

B. High-Performance Liquid Chromatography (HPLC)

As mentioned in Section A, high-performance liquid chromatography (HPLC) is a type of chromatography, specifically column chromatography. HPLC uses a column that is packed with the stationary phase; the mobile phase flows through the column. A sample is injected manually (using a syringe), or by automation (using an autosampler), into the column. Relatively high pressures are used to increase time efficiencies by decreasing retention times of solutes. A detector detects the solutes as they elute from the column. A wide variety of samples may be used in HPLC: nucleic acids, amino acids, proteins, carbohydrates, lipids, steroids, drugs, and other biologically active molecules.[1]

HPLC offers tremendous advantages over other chromatographic techniques. Resolution, the ability to discern or differentiate two similar forms of a molecule, is high. Fast analysis times in HPLC enables the examination of the data during separation. HPLC columns can be reused without repacking the stationary phase, which saves time.[1] Reproducibility, a very desirable property, is high because parameters (i.e., flow rate, mobile phase composition), that modulate partitioning efficiency, can be controlled with ease.[1] The operation of the HPLC instrument and data analysis can be automated; thus, one can simply prepare the samples, place them in an autosampler, and have the data ready quickly depending on the situation, such as number of samples.[1] Additionally, HPLC can be operated at ambient temperatures, hence decreasing the possibility of thermal destruction of the sample.[1]

One of the biggest advantages of HPLC is the different modes that can be used. For instance, HPLC can be operated in a normal-phase or reverse-phase mode. In normal-phase HPLC, the stationary phase (e.g. silica with silanol groups) is polar, while the mobile phase is non-polar. On the other hand, the stationary phase is non-polar and the mobile phase is polar in reverse-phase HPLC (RP-HPLC). Consequently, the normal-phase mode is used to separate polar, or hydrophilic, solutes and the reverse-phase mode is used to separate non-polar, or hydrophobic, solutes. Polar molecules will interact with the polar column in normal-phase HPLC, thus will be retained longer. Similarly, non-polar molecules will interact with the non-polar column in RP-HPLC, thus will be retained longer. Typical mobile phases used in normal-phase HPLC are *n*-hexane, chloroform, and chloroethane. In contrast, typical organic/aqueous solvent systems used in RP-HPLC are methanol/water, acetonitrile/water, and tetrahydrofuran/water. Today, more than 600 kinds of reverse-phase columns are commercially available worldwide.[2] Newer and better reverse-phase columns are constantly brought into the market.[2]

C. Chiral Molecules

By definition, chiral molecules are compounds that are not superimposable with their mirror images.[3] An example of a chiral object is one's left hand which is not superimposable with the right hand. In contrast to chirality, or handedness, achirality refers to objects with superimposable mirror images. Chiral molecules typically contain a central atom, called the chiral center (asymmetric center, stereogenic center), with four different substituents. Rigidity can also confer chirality. For instance, a molecule that

4

consists of two bulky groups attached by a single bond might not be able to rotate due to steric hindrance as shown in Figure 2a.

The term "enantiomers" represents non-superimposable mirror images of a chiral molecule. Figure 2b shows enantiomers of a chiral molecule. In this case, the chiral center is carbon. Enantiomers have identical physical (i.e., melting point, boiling point, solubility) and chemical properties. The one property that distinguishes enantiomers is optical activity. Optical activity is the ability of a molecule to rotate plane-polarized light. One enantiomer will rotate plane-polarized light in one direction, while the other enantiomer will rotate the plane-polarized light by the same magnitude, but in the opposite direction.

Overall, enantiomers of a molecule are named using either the R/S system or d/l (+/-) system. The R/S system is used when the absolute configuration is determined. In other words, the spatial arrangement of the substituents is used to differentiate the enantiomeric pair. By assigning priorities according to the atomic number of the substituents around the chiral center, each enantiomer is designated R or S. One priority determinant rule consists of the following steps. When starting from the highest priority substituent (highest atomic number), if the priority order is clockwise, the enantiomer is called R. In contrast, if the priority order is counterclockwise, the enantiomer is called S. Figure 2c shows an application of this priority determinant rule. In contrast, the d/l (dextrorotatory/levorotatory) system is used only after the direction of plane-polarized light rotation is determined experimentally. An enantiomer that rotates plane-polarized light to the right, or clockwise, is designated d (or +). In contrast, an enantiomer that

5

Figure 2a. Molecule that is chiral due to steric hindrance to free rotation by two bulky groups.
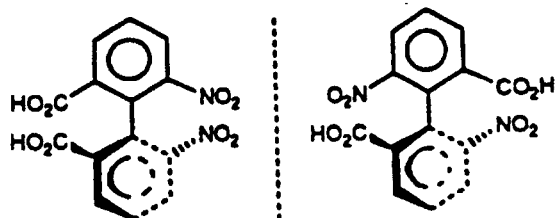
Figure 2b. Enantiomers of a chiral molecule.
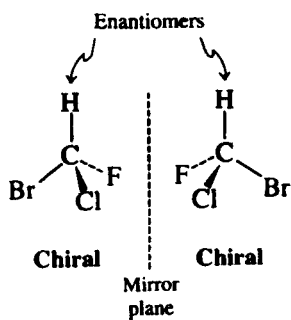
Figure 2c. Enantiomers of a chiral molecule with *R/S* designations.
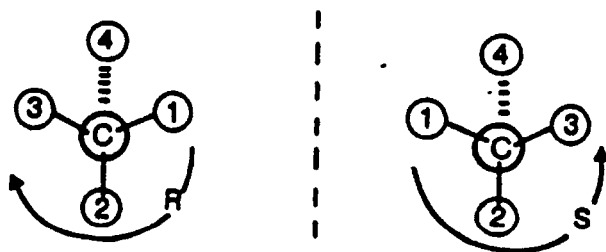
rotates plane-polarized light to the left, or counter clockwise, is designated *l* (or -). The

R/S designations only designate the spatial arrangement of the substituents, but do not

predict the direction of plane-polarized light rotation.

D. Applications of Chiral Separation

In principle, biological systems are chiral in nature. Hence, in order to separate

enantiomers in biological systems, one must be able to perform chiral separations. For

instance, enzymes are prime examples of molecules that can distinguish between the

enantiomeric forms of its target, or substrate.[5] An enzyme might only bind to the *R* form

of the substrate and not to the *S* form because of the active site's inherent chiral nature.

Chiral separations are desirable and highly marketable in the pharmaceutical industry.

For instance, in 1999, single-isomer drug sales reached $115 billion worldwide, or 32%

of the $360 billion total drug sales worldwide.[4] Chiral drugs are widely used in various

medical disciplines such as cardiovascular, endocrinology, hematology, respiratory,

gastrointestinal, dermatological, analgesics, and vaccines.[4] In the biopharmaceutical

industry, synthetic drugs are fabricated in enantiomeric forms; sometimes, one

enantiomer of a drug is safe and the other enantiomer is toxic. Therefore, the safe

enantiomer is purified and chromatography is done to determine the purity.

A classic example involves a 1970s drug called thalidomide (α-

phtalimidoglutarimide).[6] Pregnant women experienced morning sickness, with

symptoms consisting of nausea and vomiting. Thalidomide was advertised as the drug

that would counter these symptoms. The United States Surgeon General did not approve

7

thalidomide because extensive clinical trials were not performed. Surprisingly, the test subjects in the clinical trials were only of one gender and ethnicity – white male prisoners. However, European countries approved the usage of thalidomide to combat morning sickness. Disaster followed upon usage of this drug by pregnant females – babies were born with partial arms and legs or no limbs at all. Fifteen years later, a journal, called *Chirality*,[7] released mice studies that showed that D-thalidomide was the safe enantiomeric form of thalidomide for the fetus, while L-thalidomide was the harmful form. Figure 3 shows the chemical structure of thalidomide.

E. Methods of Chiral Separation

Scientists have devised various methods to achieve chiral separation. One such technique is enzymatic catalysis.[5] As mentioned in Section D, enzymes are biomolecules that can distinguish between the enantiomeric forms of its target. Consequently, the enzyme will bind only one enantiomeric form of the target and catalyze a reaction, resulting in a product with a specific configuration. Another chiral separation method involves adding a chiral reagent to a solution, containing enantiomers of interest, and forming diastereomers. Enantiomers are stereoisomers that are mirror images of each other; in contrast, diastereomers are stereoisomers that are not mirror images of each other. Since diastereomers have different physical properties (i.e., melting point, boiling point, solubility), they can be separated by physical means such as fractional distillation. Both of these chiral separation techniques are non-chromatographic methods that involve multiple steps, which result in low efficiency (partial separation). One technique that

Figure 3. Chemical structure of thalidomide.

Thalidomide
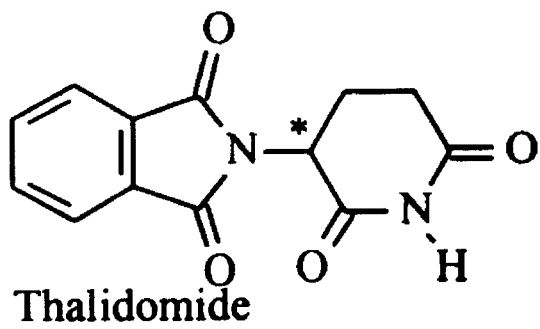
does involve chromatography utilizes the addition of a chiral selector to the mobile phase in HPLC. The chiral selector forms diastereomeric complexes with the enantiomers; these complexes will have different retention times due to differential binding to the stationary phase. Another technique that involves chromatography is reverse-phase HPLC (RP-HPLC) coupled with a chiral stationary phase (CSP). Since these stationary phases are chiral, they will interact with enantiomers differently to form diastereomeric complexes, hence partitioning the two forms of the solute. Differences in the degree and type of interactions of groups on both the CSP and the solute may result in chiral separation. Some advantages of using CSPs include simple mobile phase composition and shorter column equilibration time. Disadvantages consist of the following: limited parameters to optimize and less universal approaches.[8] In this research work, CSPs were used as the stationary phase, in conjunction with RP-HPLC, to obtain chiral separation.

F. Mechanism of Chiral Separation

In 1952, Dalgliesh postulated the "three-point rule" as the mechanism of chiral separations. The rule states that three simultaneous interactions between the chiral selector and solute must take place in order for enantioselectivity to occur. Additionally, at least one interaction of the three must depend on the stereochemistry at the chiral center of both the chiral selector and the enantiomers. The types of interactions that occur during chiral separation may consist of the following: electrostatic interactions, hydrogen bonding, van der Waals forces, dipole stacking, hydrophobic interactions, π-π interactions, steric repulsions, and formation of inclusion complexes.

Figure 4 depicts an example of the three-point rule. The molecules on the left-hand side are the chiral selectors and the molecules on the right-hand side are the enantiomers of a solute, which are designated A(+) and A(-), respectively. The stereochemistry at the chiral center of both chiral selectors is the same. On the other hand, the enantiomeric solutes have different stereochemistry. Notice that in both the top and bottom cases, three simultaneous interactions occur – electrostatic interactions and steric repulsion. The electrostatic interactions occur between the acidic and basic sites, while steric repulsion occurs between the bulky groups. In the top case, the overall degree of attractive interactions is greater due to attractive electrostatic interactions between the acidic and basic sites of the chiral selector and enantiomer, A(+). In the bottom case, the acidic and basic sites of both molecules have a greater overall degree of repulsive interactions. Hence, A(+) will be retained longer and have a longer retention time than A(-). The three-point rule enables one to qualitatively explain why an enantiomer is retained longer than the other. Overall, the degree of chiral separations is dependent on the nature of interactions and orientation/distance of interacting groups on the CSP and on the solute. The seemingly endless possibilities of CSPs and their associated chiral separation abilities have resulted in considerable interest in exploring their applications.

G. Chiral Stationary Phases (CSP)

Chiral stationary phases (CSP), used in conjunction with RP-HPLC, are powerful tools that can achieve chiral separation. CSPs consist of two components: a stationary solid support and a chiral selector. Typical stationary solid supports used are: silica,

Figure 4. An application of the three-point rule.
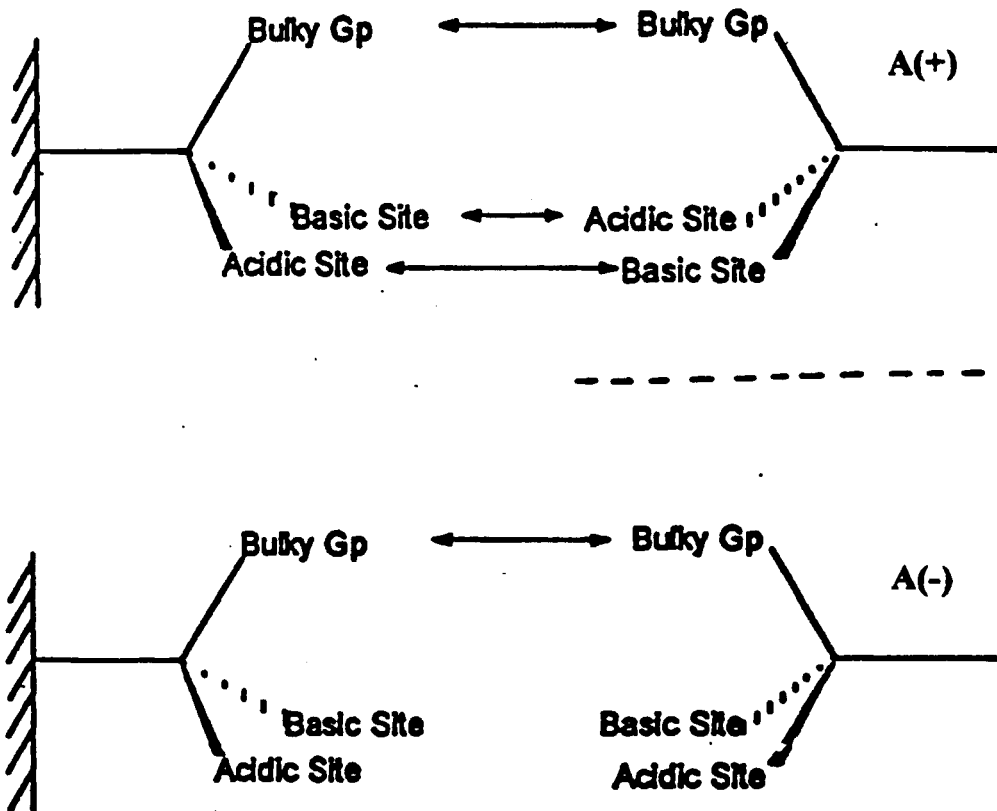
alumina, zirconia, titania, and thoria.[9] Silica is most commonly and widely used due to multiple advantages. One advantage is that the structure of silica is rigid and stable. Also, the silanol groups (Si-OH) are very accessible to modifications due to the large surface area of silica; as a result, it is easy to convert silica into various bonded phases. A wide variety of particle sizes, pore sizes, and surface areas are available. Finally, silica contains many different types of silanol groups within its structure. The most reactive silanol groups are on the surface of silica. These polar groups are responsible for interacting with the solute. Another type of silanol group is located in the internal structure of silica; this group is responsible for silica's physical characteristics such as particle size, pore size, and surface area. Figure 5 shows the structure of silica and the different types of silanol groups. However, the main disadvantage of silica is its stability range from only pH 2 to pH 8.[9] Oxides of alumina, zirconia, and thoria have a wider pH stability range.[9] In RP-HPLC, silica is modified with relatively non-polar groups (e.g. organic hydrocarbons) to create a non-polar stationary phase. The maximum amount of silanol groups that can be modified on the silica surface has been estimated to be approximately 8 μmol/m^2. The maximum surface coverage of the silica surface is approximately 4.5 μmol/m^2. As a consequence, there are still some unmodified silanol groups left after modification. In this research work, Vydac silica was used as the stationary solid support. Vydac silica has a particle size of 6.5 μm, a pore size of 300 Å, and a surface area of 106 m^2/g.

The chiral selectors used in this research work were 2-hydroxy-3-methacryloyloxypropryl-β-cyclodextrin (substituted β-cyclodextrin) and quinine. This

13

Figure 5. Structure of silica.
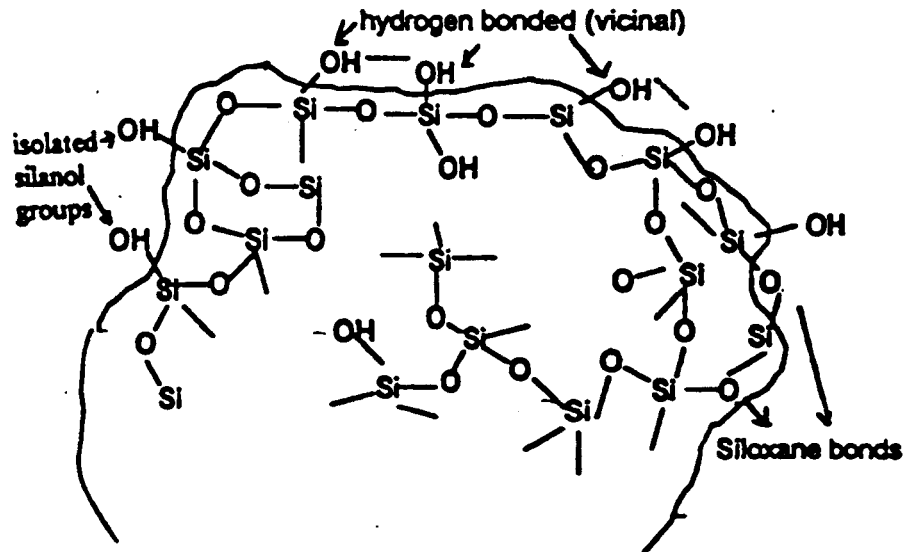
cyclodextrin form consists of hydroxyl groups that are partially modified. Native β-

cyclodextrin, or unmodified β-cyclodextrin, is a cyclic oligosaccharide, consisting of

seven D-(+) glucose residues (in a chair conformation) bonded via 1,4 alpha glycosidic

linkages. The overall structure resembles a cone that has a mouth and a base. The mouth

is larger than the base. Fixed hydroxyl groups are located at the mouth, while free

hydroxyl groups reside in the base. The base is partially blocked due to the ability of the

free hydroxyl groups to freely rotate. The interior of the cone is designated as a

hydrophobic cavity due to the absence of hydroxyl groups. Native cyclodextrin can exist

in three different forms: α-, β-, and γ-cyclodextrin. The differences between these forms

stem from the number of glucose residues. The physical properties of the different forms

are summarized in Table 1. Cyclodextrin achieves chiral separation through electrostatic

interactions, hydrogen bonding, dipole stacking, hydrophobic interactions, steric

repulsions, and formation of inclusion complexes. For example, as the solute enters the

hydrophobic cavity, an inclusion complex between cyclodextrin and the solute forms.

Moreover, non-polar groups on the solute interact with the hydrophobic cavity. Hence,

as one attempts to qualitatively explain data using a cyclodextrin column, one must look

at factors that favor/disfavor inclusion complex formation – size, polarity, and shape of

the solute with respect to cyclodextrin. Figures 6 and 7 show the structure of native β-

cyclodextrin from a molecular standpoint and an illustrative standpoint, respectively.

Quinine is a relatively new chiral selector that has shown to be stable and offers high

separation efficiency.[10] Figure 8 shows the structure of quinine. Certain types of

aliphatic and aromatic alcohols (i.e.anthryltrifluoroethanol, 2-methyl-1-phenyl-1-

Table 1. Native cyclodextrin forms and physical properties.

native cyclodextrin forms	# glucose residues	molecular weight (g/mol)	hydrophobic cavity diameter (Å)		
			external	internal	depth
α	6	973	13.7	5.7	7.8
β	7	1135	15.3	7.8	7.8
γ	8	1297	16.9	9.5	7.8

Figure 6. Structure of native β-cyclodextrin (molecular standpoint).
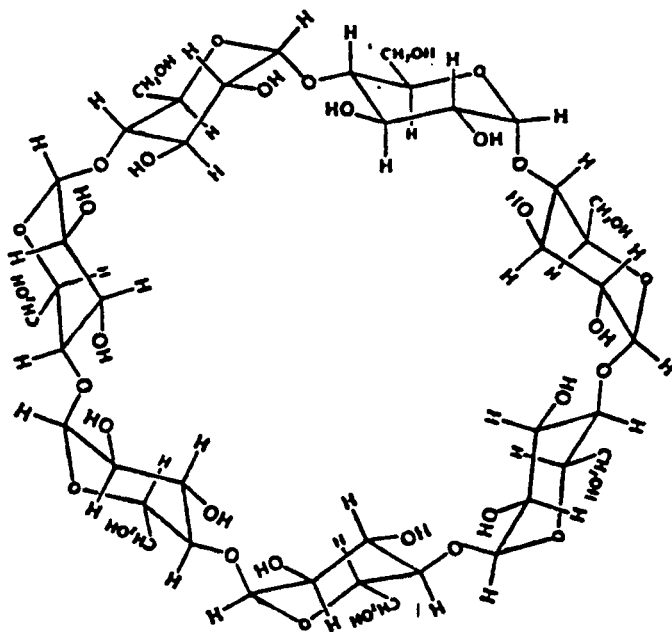
Figure 7. Structure of native β-cyclodextrin (illustrative standpoint).
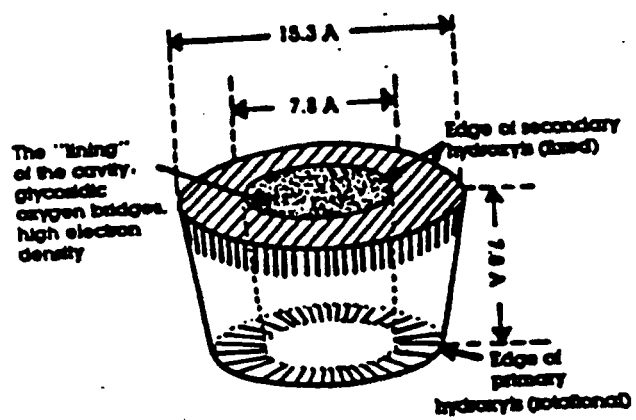
propanol, binaphthol) and their enantiomers have been partitioned using quinine.[10] In this research, various solutes were run on the 2-hydroxy-3-methacryloyloxypropyl-β-cyclodextrin and quinine columns to compare separation abilities.

There exists a classification scheme according to the type of CSP-solute complexes formed and interactions between the CSP and the solute: chiral ligand exchange chromatography, synthetic multiple interaction CSPs (Pirkle type bonded phases), protein CSPs, cellulose CSPs, and cyclodextrin CSPs. In the chiral ligand exchange chromatography classification, the solute binds to the ligand, which is attached to the stationary solid support, in the presence of metal cations in the mobile phase. The resulting CSP-solute complex is a diastereomeric chelate complex. The synthetic multiple interaction CSP (Pirkle type bonded phases) is a classification scheme based on the three-point rule that was discussed earlier. The protein CSP classification involves attaching a protein (i.e., albumin, α-acid glycoprotein, bovine serum albumin (BSA)) to the stationary solid support. A protein has a great potential to act as a chiral selector due to its strong interactions with negatively-charged, inorganic, and organic compounds via electrostatic interactions, hydrogen bonding, hydrophobic interactions, and charge transfer processes. A disadvantage of the protein CSP is the requirement of high pH conditions. The cellulose CSP involves cellulose, or its derivatives, acting as the chiral selector. Upon interaction, the solute forms an inclusion complex within the helical structure of the polysaccharide.

Figure 8. Structure of quinine.
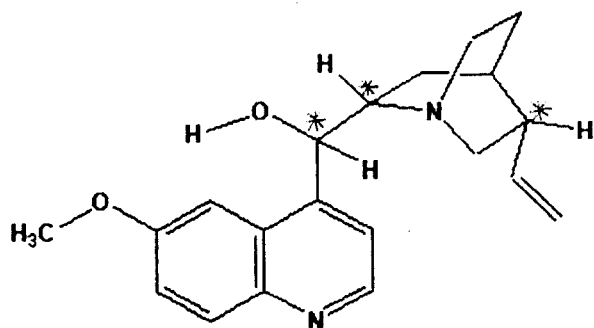
H. Methods of CSP Synthesis

As mentioned in Section G, if silica is selected as the stationary solid support, it is easy to convert it into various bonded phases. Many reaction types have been devised to synthesize CSPs from the silanol groups on silica. One reaction type is esterification.[9] In this reaction, a silanol reacts with an alcohol to form a Si-O-C surface linkage. This was the first reaction type used to fabricate bonded phases. Unfortunately, the Si-O-C surface linkage is hydrolytically unstable; hence, the bonded phase produced by esterification cannot be used in aqueous conditions. Figure 9 shows the esterification reaction.

The second reaction type is called organosilanization; this is still the preferred and widely used method to create a CSP.[9] The two approaches to achieve organosilanization are depicted in Figure 9. The first approach involves a silanol reacting with an organosilane reagent with one reactive group (X). Typically, X is chlorine, methoxy, or ethoxy. The resulting CSP is monomeric in nature – each silanol group contains one organic moiety. The second approach involves a silanol reacting with an organosilane reagent with three reactive groups (X). Again, X is chlorine, methoxy, or ethoxy. The resulting CSP is polymeric in nature; the organic moieties of each silanol group are cross-linked. The monomer reaction is experimentally more reproducible than the polymer reaction. The resulting surface bonds from organosilanization is a Si-O-Si-C surface linkage. One disadvantage of this surface linkage is its instability at extreme conditions (e.g. pH < 2 and pH > 8). Another disadvantage is organosilanization can result in low surface coverage, which may result in greater tailing of peaks.

The third reaction type is a two-step process: chlorination followed by reaction of

21

Figure 9. Reaction types.

REACTION TYPE	REACTION	SURFACE LINKAGES
ESTERIFICATION	Si - OH + R - OH → Si - OR + H₂O	Si - O - C
ORGANO-SILANIZATION	a).Si - OH + X - SiR'₂R → Si - O - SiR'₂R + HX b).Si - OH + X₃ - Si - R → Si - O - Si - R + 3HX Y = Si or H OY	Si - O - Si - C
CHLORINATION FOLLOWED BY REACTION OF GRIGNARD REAGENTS AND ORGANOLITHIUM COMPOUNDS	Si - OH + SOCl₂ →(Toluene) Si - Cl + SO₂ + HCl a). Si - Cl + BrMgR → Si - R + MgClBr or b). Si - Cl + Li - R → Si - R + LiCl	Si - C
a). TES SILANIZATION	a).	a). Si - H monolayer
b). HYDROSILATION	b).Si - H + CH₂ = CH - R →(Catalyst) Si - CH₂ - CH₂ - R	b). Si - C

For the TES SILANIZATION row (a):

```
    |             |             |
    O             O             O
    |             |             |
 - Si - OH      - Si - O - Si - H
    |             |             |
    O             O             O
    |             |             |
 - Si - OH   →  - Si - O - Si - H
    |             |             |
    O             O             O
    |             |             |
 - Si - OH      - Si - O - Si - H
    |             |             |
    O             O             O
    |             |             |
```

22

a Grignard reagent or organolithium compound to attach the organic moiety.[9] First, the

silanol reacts with a chlorinating reagent such as thionyl chloride, $SOCl_2$, to form a Si-Cl

surface linkage. Second, Si-Cl can either react with a Grignard reagent, such as BrMgR,

to form a Si-C surface linkage or with an organolithium compound, Li-R, to similarly

form a Si-C surface linkage. Because the organic moiety of interest is directly bonded to

Si, this surface linkage is hydrolytically more stable than the Si-O-Si-C linkage formed

from organosilanization. However, extremely dry conditions must be present during

synthesis because the Si-Cl bond can be hydrolyzed to reform the silanol. Figure 9 shows

this third reaction type.

The final reaction type that can be used to synthesize chiral stationary phases is TES

silanization/hydrosilation,[9] as shown in Figure 9. In TES silanization, the silanol groups

are converted into silica hydrides, forming a Si-H monolayer. The hydroxyl groups are

replaced to form Si-H surface linkages by using a reducing reagent, such as lithium

aluminum hydride (LAH or $LiAlH_4$). Another method is by adding a reagent, such as

triethoxysilane (TES), to silanize the silica surface. TES was used in this research

project. Subsequently, the Si-H monolayer is reacted with a terminal olefin, an alkene

with a double bond at the C-1 position, in the presence of a catalyst to form Si-C surface

linkages. Hexachloroplatinic acid (Speier's catalyst) was used in the hydrosilation

rection (catalytic addition) in this research project. Other catalysts can be used as well,

such as different transition metal complexes (i.e. Pt, Rh, Pd, Ir, Ni, Cr, Ti)[11] and specific

types of free radical initiators (i.e., AIBN, t-butyl peroxide).[12,13] The most effective,

accessible, and frequently used hydrosilation catalysts are all Pt-containing, in particular

Speier's, Karstedt, and Lamoreaux catalysts.[11] The Si-C bond is more stable than the Si-O-Si-C bond; this results in longer column lifetimes and more reproducible retention times. Because the hydrosilation reaction has few inherent disadvantages, a wide variety of organic moieties may be used. For instance, the TES silanization/hydrosilation reactions diminish interference from other functional groups. The silanization/hydrosilation reaction scheme may also be used in capillary electrophoresis (CE). This scheme can also be used to bind alkyne moieties to hydride surfaces.

I. Goals

The first goal of this research project was to use new test solutes on the 2-hydroxy-3-methacryloyloxypropryl-β-cyclodextrin column (using two different organic/aqueous solvent systems: methanol/water and acetonitrile/water) as well as confirm that temazepam and oxazepam could be partitioned. The second goal was to synthesize a chiral stationary phase, using quinine as the chiral selector, by the TES silanization/hydrosilation reaction scheme and confirm reaction success by DRIFT (Diffuse Reflectance Infrared Fourier Transform) spectroscopy, ^{13}C CP-MAS NMR (Cross Polarization Magic-Angle Spinning Nuclear Magnetic Resonance) spectroscopy, and elemental analysis. The third goal was to use the same solutes in the first goal and attempt to partition the enantiomers using the quinine column (again using two different organic/aqueous solvent systems: methanol/water and acetonitrile/water). The fourth goal was to compare the 2-hydroxy-3-methacryloyloxpropryl-β-cyclodextrin column and the quinine column in terms of separation abilities and efficiencies. The final goal was to

examine pH effects on the quinine column's ability to partition and resolve enantiomeric forms of selected solutes.

CHAPTER II

EXPERIMENTAL

A. Materials

1. Chemicals

The chemicals used in this research project are listed in alphabetical order with their

Chemical Abstracts Service (CAS) registry number.

Table 2. CAS registry number of chemicals.

Chemical Name	CAS registry number
acetic acid	[64-19-7]
acetonitrile	[75-05-8]
(R)-binaphthol	[18531-94-7]
(S)-binapthol	[18531-99-2]
dibutyltin dilaurate	[77-58-7]
chlortetracycline	[64-72-2]
clenbuterol	[21898-19-1]
dioxane	[123-91-1]
diethyl ether	[60-29-7]
(R)-(-)-2,2,2-trifluoro-1-(9-anthryl) ethanol	[53531-34-3]
(S)-(+)-2,2,2-trifluoro-1-(9-anthryl) ethanol	[60646-30-2]
DL-homatropine	[51-56-9]

hydrochloric acid (HCl)	[7647-01-0]
imipramine	
methanol	[67-56-1]
(R)-(+)-2-methyl-1-phenyl-propanol	[14898-86-3]
N,O-Bis (trimethylsilyl) trifluoroacetamide	[25561-30-2]
nortriptyline	[894-71-3]
oxazepam	[604-75-1]
2-phenoxypropionic acid	[940-31-8]
2-phenyl-1,2-propanediol	[4217-66-7]
1-phenyl-2-propanol	[14898-87-4]
2-propanol	[67-63-0]
DL-propranolol	[318-98-9]
quinine	[130-95-0]
temazepam	[849-50-4]
terbutaline	[23031-32-5]
tetracycline	[60-54-8]
tetrahydrofuran (THF)	[109-99-9]
triethoxysilane (TES)	[998-30-1]
tropicamide	[1508-75-4]

2. Materials for CSP Synthesis

Vydac silica was used as the stationary solid support and has a particle size of 6.5 μm, a pore size of 300 Å, and a surface area of 106 m^2/g (Catalog # 101TPB6.5; Lot #930816-4A). First the silanol groups on Vydac silica were converted to silica-hydride monolayers by adding dioxane (Fischer Scientific; Fair Lawn, NJ), 2.3 M hydrochloric acid (HCl), and triethoxysilane (Aldrich Chemical Co.; Milwaukee, WI). The washing steps of TES silanization used tetrahydrofuran (Burdick & Jackson; Muskegon, WI) and diethyl ether (Fischer Scientific; Fair Lawn, NJ) in reagent grades. Subsequently, the silica-hydride monolayers were converted to silica-carbon surface linkages by reacting with a chiral selector, quinine (Aldrich Chemical Co.; Milwaukee, WI), and adding 2-propanol (Fischer Scientific; Fair Lawn, NJ), acetic acid (EM Science; Gibbstown, NJ), and Speier's catalyst. The washing steps of hydrosilation used 2-propanol (Fischer Scientific; Fair Lawn, NJ) and diethyl ether (Fischer Scientific; Fair Lawn, NJ) in reagent grades. The water used was of highest purity by preparation on a Milli-Q apparatus (Millipore Corp.; Bedford, MA).

B. Instrumentation
1. DRIFT (Diffuse Reflectance Infrared Fourier Transform) Spectroscopy

DRIFT spectroscopy, a type of infrared spectroscopy (specifically mid-infrared (400 – 4000 cm^{-1}), can be used as an analytical method for untreated solid (e.g. fine powdered samples) and liquid materials.[16] One advantage of DRIFT spectroscopy is that minimal

sample preparation is needed. Another advantage is data can be obtained quickly (e.g. in minutes).

The fundamental process of this type of infrared spectroscopy is diffuse reflection (a type of radiation reflection) – a complex process that results when radiation collides with the surface of a solid or liquid sample. After the collision, the radiation excites vibrational modes in the sample; the vibrational modes then scatter the light in all directions. As a result, a reflectance spectrum is produced that is unique to the sample. The reflectance of the sample is the ratio of the signal of the sample to the signal of the reference material.

DRIFT spectroscopy is typically performed on FTIR instruments due to the weak signal produced by the sample. As with most analytical methods, a reference material is used. For this technique, finely ground potassium bromide (KBr) is the reference material. Potassium bromide is used because it is a good reflector; hence, it imparts a good reference signal. Solid materials must be ground very finely until the particle size is less than the wavelength of radiation. Fourier transform is used for data processing due to better signal-to-noise (S/N) ratios. Another advantage is Fourier transform allows rapid data acquisition by simultaneously measuring all of the resolution elements for a spectrum.

In this research work, DRIFT spectroscopy was used to confirm the success of the TES silanization and hydrosilation reactions. The Mattson Infinity series FTIR spectrophotometer (Madison, WI) was used to obtain reflectance spectra of the silica samples. The whole system, consisting of the cell compartment and lines, was purged

with nitrogen gas at 25-30 psi for approximately 25 minutes before measurement to eliminate CO_2 and H_2O. Without purging, CO_2 and H_2O peaks will appear in the DRIFT spectrum and obscure some sample peaks. A flat and uniform surface is needed to perform DRIFT spectroscopy; thus, a spatula was used to flatten the surface of the reference material and sample to ensure uniformity after placing the reference material or sample into the small metal cup of a plastic sample holder.

The infrared spectrum of KBr was scanned 100 times at a resolution of 4 cm^{-1} from 4000 cm^{-1} to 450 cm^{-1}. The sample preparation was relatively simple. First, approximately 100 mg of the silica sample was measured into a small cylindrical glass container that was dried overnight in an oven at 80°C. Then, 5 mg of KBr (5% of 100 mg) was mixed with the silica sample. After mixing, the sample was dried overnight in an oven at 80°C. The sample then was placed into the small metal cup. Next, the plastic sample holder was placed into the cell compartment of the FTIR instrument. The infrared spectrum of the silica sample was scanned 100 times at a resolution of 4 cm^{-1} from 4000 cm^{-1} to 450 cm^{-1}. The signal was obtained as % transmittance. The data was analyzed by a computer using the software package Winfirst.

2. ^{13}C CP-MAS NMR (Cross Polarization Magic-Angle Spinning Nuclear Magnetic Resonance) Spectroscopy

^{13}C CP-MAS NMR spectroscopy, a type of ^{13}C NMR, is similar to ^{1}H NMR. One difference is ^{13}C NMR provides information about the backbone of a molecule instead of information of the attached hydrogens of the molecule. Another difference is ^{13}C NMR signals occur 0-200 δ (chemical shift), or ppm (parts per million), downfield from the

carbon peak of tetramethylsilane (TMS), a reference molecule, instead of 0-12 δ from the hydrogens of the same compound. Consequently, there is less overlap of peaks. Because only 1.1% of carbon atoms are ^{13}C, a significantly larger sample must be utilized and coupling between carbon atoms is not common. ^{13}C CP-MAS NMR spectroscopy is classified to as a type of solid state NMR spectroscopy.

In the past, ^{13}C NMR was not useful for solid samples due to line broadening – this phenomenon masks the distinct NMR peaks.[16] Chemical shift anisotropy can cause line broadening in solids. However, magic angle spinning (MAS) eliminates chemical shift anisotropy by rotating solid samples at extremely high frequencies (> 2 kHz). In order to take advantage of this phenomena, the solid sample is placed in a special sample holder that is maintained at an angle of 57.4° with respect to the applied magnetic field. Overall, the rotation in the applied magnetic field allows the solid sample to have liquid-like behavior.

Cross polarization (CP) is used to eliminate long spin-lattice relaxation times.[16] Long spin-lattice relaxation times for excited ^{13}C nuclei is a limiting factor in ^{13}C CP-MAS NMR of solid materials. Upon excitation, the ^{13}C nuclei returns to its equilibrium ground state within a period of time, called the spin-lattice relaxation time. However, the relaxation time of ^{13}C nuclei in solids is long, on the order of minutes. As a result, in order to obtain a good spectrum, long periods of time (i.e., hours or days) are needed. Cross polarization solves this dilemma by ultimately hastening the spin-lattice relaxation time of the ^{13}C nuclei through the interactions with the magnetic fields of proton nuclei.

^{13}C CP-MAS NMR spectra were obtained on a NMR-Varian JNOVA 400 MHz spectrometer. The solid silica sample was spun at a frequency of 5000 Hz. Glycine was used as the standard. A Sun computer was used to analyze the data.

3. Elemental Analysis

Elemental analysis is a method used to analyze a sample for specific elements such as carbon, hydrogen, oxygen, sulfur, and nitrogen.[16] Automated instruments have been designed to accomplish elemental analysis; the underlying concept that these instruments operate under is thermal conductivity detection. The mechanism of elemental analysis is combustion. The sample, an organic compound, is oxidized at a high temperature; this process converts the sample into the elements of interest in a gaseous state, such as CO_2 or water. The automated instrument determines the percentage of certain elements present based on the mass of the sample.

The hydrosilation sample in this research was shipped to Desert Analytics (Tucson, AZ) to determine the percentage of carbon present. From the percentage of carbon present, one can calculate the surface coverage, α_R, of the bonded groups, or organic moieties. The surface coverage is empirically determined by using the following equation - α_R ($\mu mol/m^2$) = 10^6 P_c / (100 $M_c n_c$ – $P_c M_R$) S_{BET}. P_c is the carbon percentage difference between the hydrosilation product and the silica hydride. M_c and M_R are the molar masses of carbon and bonded groups, respectively. n_c is the number of carbons in the bonded groups. S_{BET} is the specific surface area of the silica hydride starting

material; the Brunauer, Emmet, and Teller nitrogen adsorption method determines this parameter.

4. Column Packing

The Vydac silica-quinine chiral stationary phase was packed into an Alltech stainless steel column (Deerfield, IL) with an internal diameter of 4.6 mm × 150 mm. Stainless steel is used to withstand the relatively high pressures of column packing and HPLC. With respect to the column packing procedure, 2 g of the chiral stationary phase was weighed out and put into a 50 mL beaker. Then, a sufficient volume of 10:90 (v/v) methanol:CCl_4 was added, in the hood, to the Vydac silica-quinine CSP; carbon tetrachloride (CCl_4) ensures the even distribution of the chiral stationary phase due to its similar density to silica. After mixing, the solution was sonicated for 10 minutes. Next, the mixture was poured into an upper reservoir of a Haskell Pump (Burbank, CA) column packer after the Alltech stainless steel column, with a large metal adaptor, was attached at the bottom of the column packer. HPLC grade methanol was then poured into the upper reservoir; methanol was used as the solvent in the packing process. The column was packed at a pressure of 5000 psi for 10-15 minutes. A fiberglass shield was placed in front of the column packer apparatus for safety reasons. Afterwards, the pump was shut off and the column was allowed to sit for 30 minutes to allow the chiral stationary phase to return to atmospheric pressure. Finally, the column was capped and transferred to an HPLC apparatus for overnight conditioning at a flow rate of 0.1 mL/min.

5. High-Performance Liquid Chromatography (HPLC)

Most HPLC instruments contain multiple components such as a solvent reservoir, solvent filters, a high-pressure pump, an autosampler/injector, a column, a detector, and a data recorder (computer). Newer instruments contain an autosampler, a device that injects multiple samples from HPLC sample vials. In contrast, older model instruments have an injector – a syringe is used to inject the sample into the HPLC system through the injector. The major disadvantage of having an injector instead of an autosampler is a set of samples must be injected manually. Consequently, the operator must perform each injection. The solvent reservoir contains the solvent system that acts as the mobile phase. The solvent is degassed prior to running the HPLC system because bubbles, created by unwanted dissolved gases (e.g. O_2), may be present and may interfere with detection or pump operation. One method of degassing is purging with an inert gas such as helium. Other methods include manually degassing with a vacuum and sonication, respectively. Solvent filters are required to remove particulate matter; this prevents accumulation in the pump and column. The pump generates relatively high pressure to attain short elution times. The detector uses ultraviolet (UV) light to monitor solute elution from the column. Finally, a recorder or computer provides separation information and enables the operator to analyze the data during and after the run.

Two different HPLC instruments were used in analyzing the 2-hydroxy-3-methacryloyloxypropyl-β-cyclodextrin and quinine columns. The first HPLC system was a Hewlett-Packard (HP) series 1050 system which consisted of a ternary pumping system. This set-up consisted of a solvent reservoir, solvent filters, a high-pressure

34

pump, an autosampler, a column, a UV detector, and a recorder (computer). A hood was not needed for this apparatus. The chromatograms were plotted using HP ChemStation software. The mobile phase components were kept in two 500 mL bottles and mixed by the system. The flow rate ranged from 0.4 mL/min to 0.5 mL/min depending on the backpressure from the column. The maximum pressure of the system without the UV detector is 400 bar, while the maximum pressure with the UV detector is 120 bar. All the samples, with the exception of one, were detected at a wavelength of 254 nm. $[Ru(bipy)_3]^{2+}$ was detected at 280 nm. The samples, in glass HP HPLC sample vials, were injected by the autosampler; each vial contained a total volume of 1 mL. The solvent system was degassed using helium at approximately 20 psi. Nitrogen was used at approximately 80 psi. Before entering the HPLC system, the solvent was filtered through a 0.20 μm mylon membrane filter. This system was used only on the 2-hydroxy-3-methacryloyloxypropyl-β-cyclodextrin column using methanol/water as the mobile phase.

The second HPLC instrument was a Waters system, which consisted of a Waters 515 HPLC pump, an injector, and a Waters 991 Photodiode Array Detector. This system consisted of a solvent reservoir, solvent filters, a high-pressure pump, an injector, a column, a UV detector, and a recorder (computer). This instrument required a hood due to the volatility of acetonitrile. The chromatograms were plotted using the Millennium (Version 2.15) Express software. The solvent was degassed by sonication for 30 minutes. The mobile phase components were mixed manually, prior to running, in 1 L bottles. The flow rate was fixed at 0.5 mL/min due to the absence of backpressure problems. The

samples were introduced through the injector, which contained a 20 µL sample loop. Before entering the HPLC system, the solvent was filtered through a Whatman 40 µm Nylon filter. This system was used on the 2-hydroxy-3-methacryloyloxypropyl-β-cyclodextrin column using acetonitrile/water as the mobile phase and on the quinine column with both methanol/water and acetonitrile/water as the mobile phase. Both mobile phases varied in composition from 90:10 (v/v) to 40:60 (v/v). Ultra pure water, made on a Milli Q apparatus, was used.

Before using any column for the first time, overnight conditioning with the appropriate solvent system at a flow rate of 0.1 mL/min was done to ensure a stable baseline. The next day, the column was equilibrated at the desired flow rate for 30-60 minutes before running any samples. Once both the pressure and absorbance were stable and resulted in flat baselines, samples were injected. The first sample run was a reference solute, such as potassium nitrate (KNO_3) or uracil. The reference is a solute that is not retained by the column – a sharp peak in the chromatogram should appear and designates the void volume. After the reference run was completed, subsequent sample runs were performed. After the runs had been completed, the column was flushed with 100% methanol for ten minutes at the normal flow rate to extend the life of the column.

The HPLC system was operated in the reverse-phase mode. Water is more polar than methanol, which in turn is more polar than acetonitrile. Therefore, acetonitrile is a stronger solvent than methanol in the reverse-phase mode and methanol is stronger than water. If the injected solute is non-polar, the stronger the solvent, the shorter the retention time – the solute elutes from the column faster. Potassium nitrate (KNO_3) or

36

uracil in methanol was used as the reference solute to determine the void time, t_o, of the columns. It was later found that there were some interactions between KNO_3 and the substituted β-cyclodextrin column, which resulted in broad peak features. Hence, uracil was used in later runs. A sample volume of 4 μL was used in the Hewlett Packard (HP) series 1050 system, while a sample volume of 20 μL was used in the Waters system. Each sample vial consisted of approximately 500 μg of solute and 1 mL of methanol. When two sample vials contained enantiomers of a solute, 500 μL of each enantiomer (in methanol) were combined in a new sample vial.

C. CSP Synthesis Procedures

1. 1.0 mM Triethoxysilane (TES) Preparation

Triethoxysilane synthesis was performed the same day that the TES silanization reaction took place. All the glassware used to prepare TES was dried for at least three hours in an oven at 80 °C. Since TES can polymerize easily when exposed to air, Argon gas was used to create an inert environment. To make a 1.0 mM TES solution in dioxane, 9.3 mL of 5.326 M TES stock solution was diluted to 50 mL with dioxane in a 50 mL volumetric flask and mixed well by inverting. The 5.326 M TES stock solution was flushed with Argon gas prior to use. Similarly, after the 1.0 mM TES solution was made, the stock solution was flushed again with Argon gas, sealed, and placed in a dessicator for storage. After preparation, the 1.0 mM TES solution was stable for approximately two hours.

2. TES Silanization

The TES silanization reaction was used to create silica-hydride surface linkages from the silanol groups on Vydac silica. First, all the glassware and 9.2632 g of Vydac silica were dried overnight in an oven at 80 °C. The glassware included a 500 mL three-necked round bottom flask, addition funnel, condenser, and drying tube. The drying tube minimizes moisture levels during the reaction procedure. The next day, the TES silanization apparatus was assembled under a hood. The apparatus consisted of a 500 mL three-necked round bottom flask, an addition funnel, a condenser, a drying tube, a thermometer, a rubber thermometer adapter, a heating mantle, a magnetic stirrer, and a magnetic stir bar. Approximately 50 mL of dioxane was put into the three-necked round bottom flask. Next, 9.2632 g of dried Vydac silica was added to the flask. The rest of the 250 mL dioxane was added to the flask in order to rinse any Vydac silica adhering to the neck of the flask. Next, 9.26 mL of 2.3 M HCl solution was added to the flask. 9.59 mL of 12 M HCl stock solution was slowly added to 40.41 mL of H_2O to a total volume of 50 mL to make the 2.3 M HCl solution. The mixture was stirred and heated for one hour at 93 °C. After the one hour incubation period, 41.66 mL of the 1.0 M TES solution was added dropwise to the flask from the addition funnel for approximately 25-30 minutes. After the addition of TES was completed, the mixture was stirred and heated for 90 minutes at 93 °C. After this second incubation period, the mixture was poured into centrifuge tubes and centrifuged for 10 minutes at 1500 rpm using an IEC HN-S centrifuge system. The supernatant, which contained dioxane and TES, was poured off into a waste beaker. The remaining material, Vydac silica hydride, was subjected to three

washings: two times with tetrahydrofuran, two times with 75:25 (v/v)

tetrahydrofuran:H$_2$O, and two times with diethyl ether. After the two washings with

tetrahydrofuran, it is possible to stop and proceed with the subsequent washings the next

day. Caution was used due to the explosive properties of diethyl ether. In each washing

step, 15 mL of the specific solvent was added to each of the centrifuge tubes with the

Vydac silica hydride, gently stirred for 10 minutes, centrifuged for 10 minutes at 1500

rpm, and the supernatant poured off into a waste beaker. After the three washings were

completed, the centrifuge tubes with the Vydacc silica hydride and small amounts of

diethyl ether were left in the hood overnight to allow the diethyl ether to evaporate. The

next day, the material was collected into a small cylindrical glass container and dried in a

vacuum oven overnight at 110 °C. Figure 10 summarizes the silanization reaction

scheme.

3. Speier's Catalyst Preparation

A previously prepared 10 mM Speier's catalyst solution was used in the hydrosilation

reaction. This solution was kept in the freezer. The solution was made by first weighing

out 0.0400 g of solid hexachloroplatinic acid hexahydrate. This was done in an inert

environment using nitrogen gas due to the high reactivity of the solid with air. Then, the

solid was dissolved with 100 mL of 2-propanol in a volumetric flask and mixed well.

4. Hydrosilation

The hydrosilation reaction was used to create silicon-carbon linkages from the silica-

hydride surface linkages on the Vydac silica hydride. First, all the glassware and

2.8154 g of Vydac silica hydride were dried overnight in an oven at 80 °C. The glassware included a 50 mL three-necked round bottom flask, addition funnel, condenser, and drying tube. The drying tube minimizes moisture levels during the reaction procedure. The next day, the hydrosilation apparatus was assembled under a hood. The apparatus consisted of a 50 mL three-necked round bottom flask, an addition funnel, a condenser, a drying tube, a thermometer, a rubber thermometer adapter, a heating mantle, a magnetic stirrer, and a magnetic stir bar. The third neck of the flask was closed with a glass stopper. Glass-to-glass contacts were sealed tightly with petroleum gel to prevent evaporation loss. 373.2 mg of quinine, 10 mL of 2-propanol, 115 μL of acetic acid, and 250 μL of 10 mM Speier's catalyst solution was sequentially added to the flask. Speier's catalyst functioned in the activation of quinine for modification. The mixture in the flask was stirred and heated for one hour at 75 °C; the solution became clear after this incubation period. After the one hour incubation period, 2.8154 g of the dried Vydac silica hydride was slowly added. The mixture was stirred and heated for 96 hours (4 days) at 75 °C. Previously, when a temperature of 80 °C was used on 2.5 g of Vydac silica hydride, evaporation loss was high. After setting the reaction temperature at 75 °C and sealing the glass-to-glass contacts with petroleum gel, evaporation loss was almost non-existent. Each day, the temperature was monitored at least three times to ensure isothermal conditions. After this long reaction period, the mixture was poured into centrifuge tubes and centrifuged for 10 minutes at 1500 rpm using an IEC HN-S centrifuge system. The supernatant was poured off into a waste beaker. The hydrosilation product was subjected to two washings: five times with 2-propanol and

Figure 10. TES silanization reaction scheme.

dry all glassware and Vydac silica in oven (80 °C; overnight)

↓

assemble TES silanization apparatus under a hood

↓

add approximately 50 mL of dioxane to three-necked round bottom flask

↓

add dried Vydac silica

↓

add rest of dioxane

↓

add 2.3 M HCl

↓

stir/incubate (93 °C; 1 hr)

↓

add 1.0 M TES dropwise (25-30 min)

↓

stir/incubate (93 °C; 90 min)

↓

wash with tetrahydrofuran (2×)

↓ can stop here

wash with 75:25 (v/v) tetrahydrofuran:H_2O (2×)

↓

wash with diethyl ether (2×)

↓

evaporate in hood (overnight)

↓

dry in vacuum oven (110 °C; overnight)

two times with diethyl ether. Caution was used due to the explosive properties of diethyl

ether. In each washing step, 15 mL of the specific solvent was added to each of the

centrifuge tubes with the hydrosilation product, gently stirred for 10 minutes, centrifuged

for 10 minutes at 1500 rpm, and the supernatant poured off into a waste beaker. After the

two washings were completed, the centrifuge tubes with the hydrosilation product and

small amounts of diethyl ether were left in the hood overnight to allow the diethyl ether

to evaporate. The next day, the product was collected into a small cylindrical glass

container and dried in a vacuum oven overnight at 110 °C. Figure 11 summarizes the

hydrosilation reaction scheme.

Figure 11. Hydrosilation reaction scheme.

dry all glassware and Vydac silica hydride in oven (80 °C; overnight)
↓
assemble hydrosilation apparatus under a hood
↓
add quinine to three-necked round bottom flask
↓
add 2-propanol
↓
add acetic acid
↓
add 10 mM Speier's catalyst
↓
stir/incubate (75 °C; 1 hr)
↓
add dried Vydac silica hydride slowly
↓
stir/incubate (75 °C; 96 hrs)
↓
wash 2-propanol (5×)
↓
wash with diethyl ether (2×)
↓
evaporate in hood (overnight)
↓
dry in vacuum oven (110 °C; overnight)

CHAPTER III

RESULTS AND DISCUSSIONS

The chiral selector, quinine (with a terminal olefin group), was attached to the

modified stationary solid support, Vydac silica hydride, by hydrosilation. Before this

reaction, the modified stationary solid support was synthesized by TES silanization using

Vydac silica. The success of both reactions was determined by DRIFT (Diffuse

Reflectance Infrared Fourier Transform) spectroscopy, ^{13}C CP-MAS NMR (Cross

Polarization Magic-Angle Spinning Nuclear Magnetic Resonance) spectroscopy, and

elemental analysis. RP-HPLC was used with both columns, 2-hydroxy-3-

methacryloyloxypropyl-β-cyclodextrin and quinine modified silica gel, were tested under

RP-HPLC conditions with methanol/water and acetonitrile/water as the solvent systems.

Samples used in this research work consisted of solutes previously used on the 2-

hydroxy-3-methacryloyloxypropyl-β-cyclodextrin column, solutes used other quinine

columns,[10] novel selenium solutes graciously donated by Dr. Kesler's research group at

San Jose State University, and a variety of drugs.

A. DRIFT Spectra for TES Silanization

Figure 12 depicts the DRIFT spectrum of the Vydac silica hydride. TES silanization

results in Si-H surface linkages that can be seen in a DRIFT spectrum. The Si-H linkage

can be seen at approximately 2250 cm^{-1}. This intense peak indicates the presence of

silica-hydride bonds at the surface of the stationary solid support. Conversely, Si-OH

surface linkages can also be seen on a DRIFT spectrum; the OH group can be seen at approximately in the range of 3550 cm^{-1} to 3750 cm^{-1} indirectly representing the Si-OH bond. Silica is heterogenous on the surface; most of the absorbance in this range is due to water adsorbed on the surface. The small sharp peak at 3750 cm^{-1} is due to the silanol groups on the surface that were not modified during the TES silanization reaction. The sharp peak at 2255.22 cm^{-1} represents the existence of Si-H surface linkages after modification of the silanol groups on Vydac silica. Consequently, TES silanization was successful.

B. DRIFT Spectra for Hydrosilation of Quinine on Vydac Silica Hydride

Figure 13 depicts the DRIFT spectrum of the Vydac silica-quinine hydrosilation product after the 96 hours reaction period. Hydrosilation results in the presence of C-H bonds, from quinine, that can be seen on a DRIFT spectrum. The C-H bond can be seen in the range of 2800 cm^{-1} to 3000 cm^{-1}. This particular peak indicates the presence of the organic moiety attached to the surface of the stationary solid support. Si-H bonds can also be seen on a DRIFT spectrum; the Si-H bond can be seen at approximately 2250 cm^{-1}. This peak shows the existence of silica-hydride bonds on the surface of the stationary solid support that were not modified during the hydrosilation reaction. Additionally, the absence of any peaks at approximately 3750 cm^{-1} shows the absence of silanol groups. There are no peaks at 2800 cm^{-1} to 3000 cm^{-1}; hence, hydrosilation was not successful. Later, it was found that between the one hour and 96 hours reaction periods, the solvent evaporated due to leakages at the glass-to-glass interfaces. The solution to this problem

was to apply petroleum gel to seal the glass-to-glass interfaces. Figure 14 depicts the

DRIFT spectrum of the Vydac silica-quinine hydrosilation product after petroleum gel

application. The C- H peak at 2980.13 cm^{-1} demonstrates the success of hydrosilation,

while the Si-H peak 2255.11 cm^{-1} shows that some silica-hydride surface linkages were

not modified.

C. ^{13}C CP-MAS NMR Spectra for Hydrosilation of Quinine on Vydac Silica Hydride

Figure 15 shows the ^{13}C CP-MAS NMR spectrum of solid quinine. The peaks

between 20 ppm and 80 ppm represent aliphatic carbons, while peaks between 100 ppm

and 220 ppm represent aromatic carbons. Figure 16 shows the spectrum for the

hydrosilation product. The peaks between 20 and 80 ppm represent aliphatic carbons;

The lack of peaks between 100 ppm and 220 ppm implicate a change in NMR relaxation

times. Because of quinine's major aromatic character, the adjacent aromatic groups tend

to associate with each other, which changes the relaxation time. Since the rings overlap,

there is a restriction in movement and a loss in signal. This phenomenon has been

observed before.

D. Elemental Analysis

The percentage of carbon present in the hydrosilation product was determined from

elemental analysis. From this value, the surface coverage, α_R, can be calculated. Surface

coverage is a parameter that quantitatively indicates how well the silica surface was

modified by the chiral selector. The greater the amount of a chiral selector successfully

Figure 12. DRIFT spectrum for Vydac silica hydride.
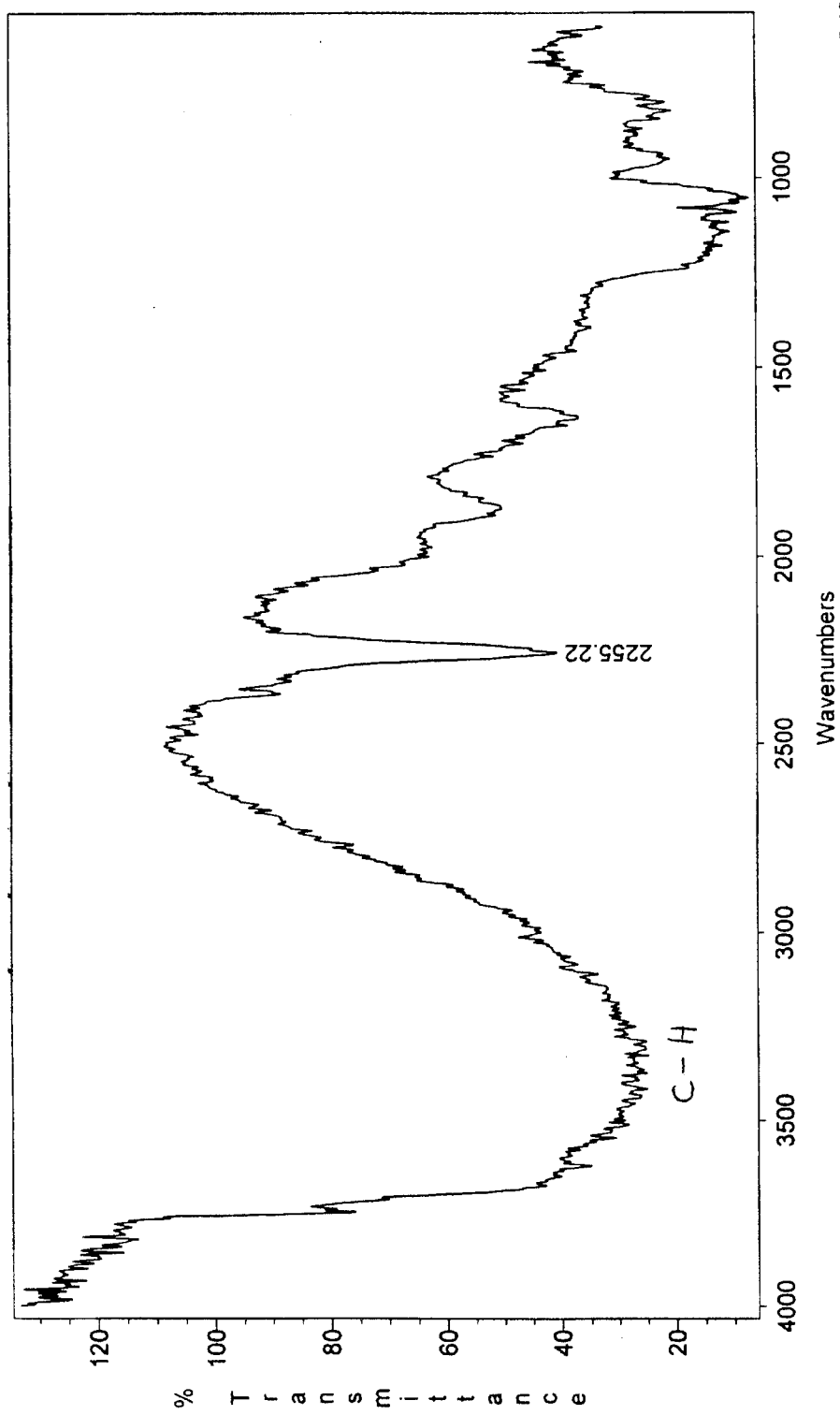
Figure 13. DRIFT spectrum for quinine bonded to Vydac silica hydride after 96 hours reaction period (before petroleum gel application).
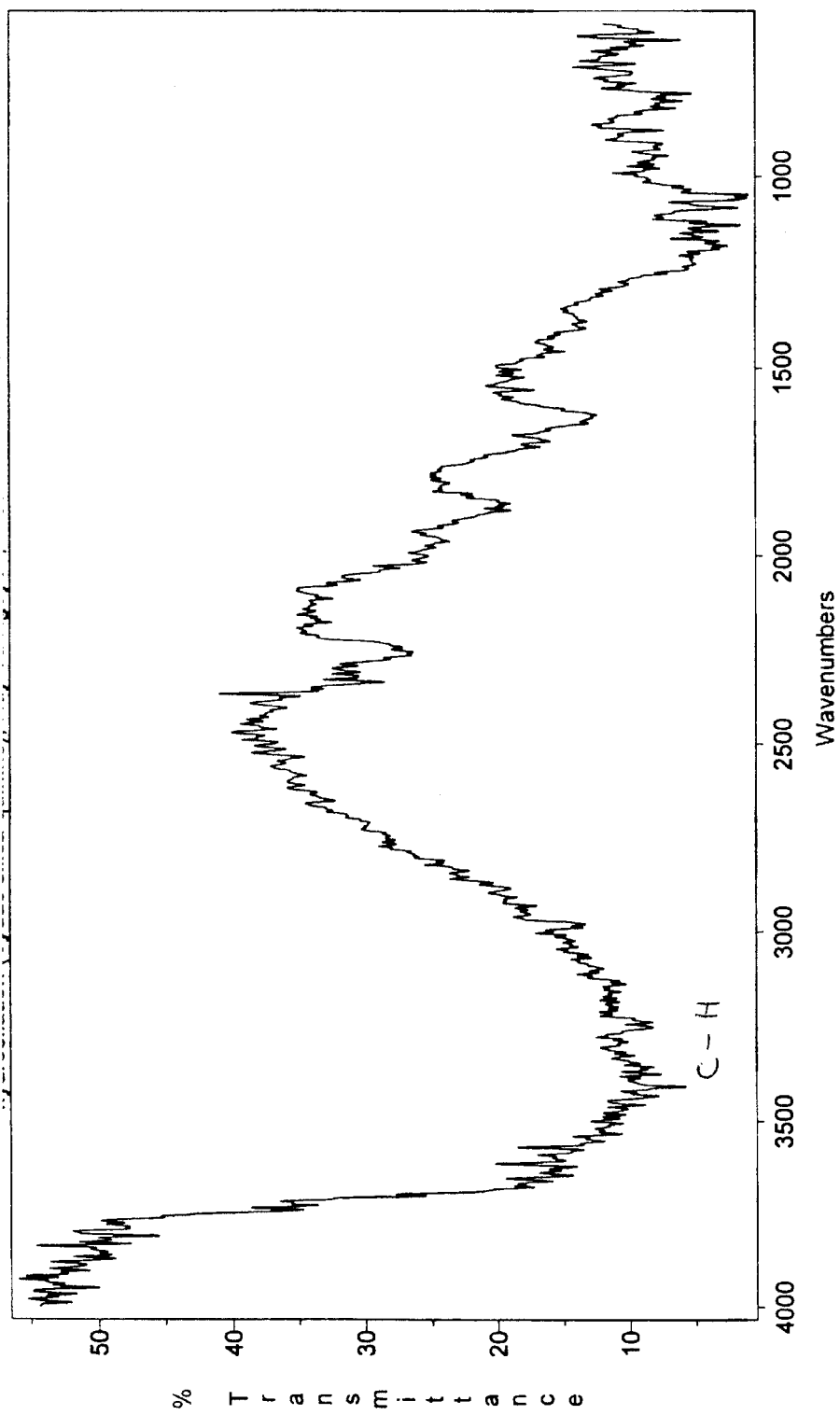
Figure 14. DRIFT spectrum for quinine bonded to Vydac silica hydride (after petroleum gel application).
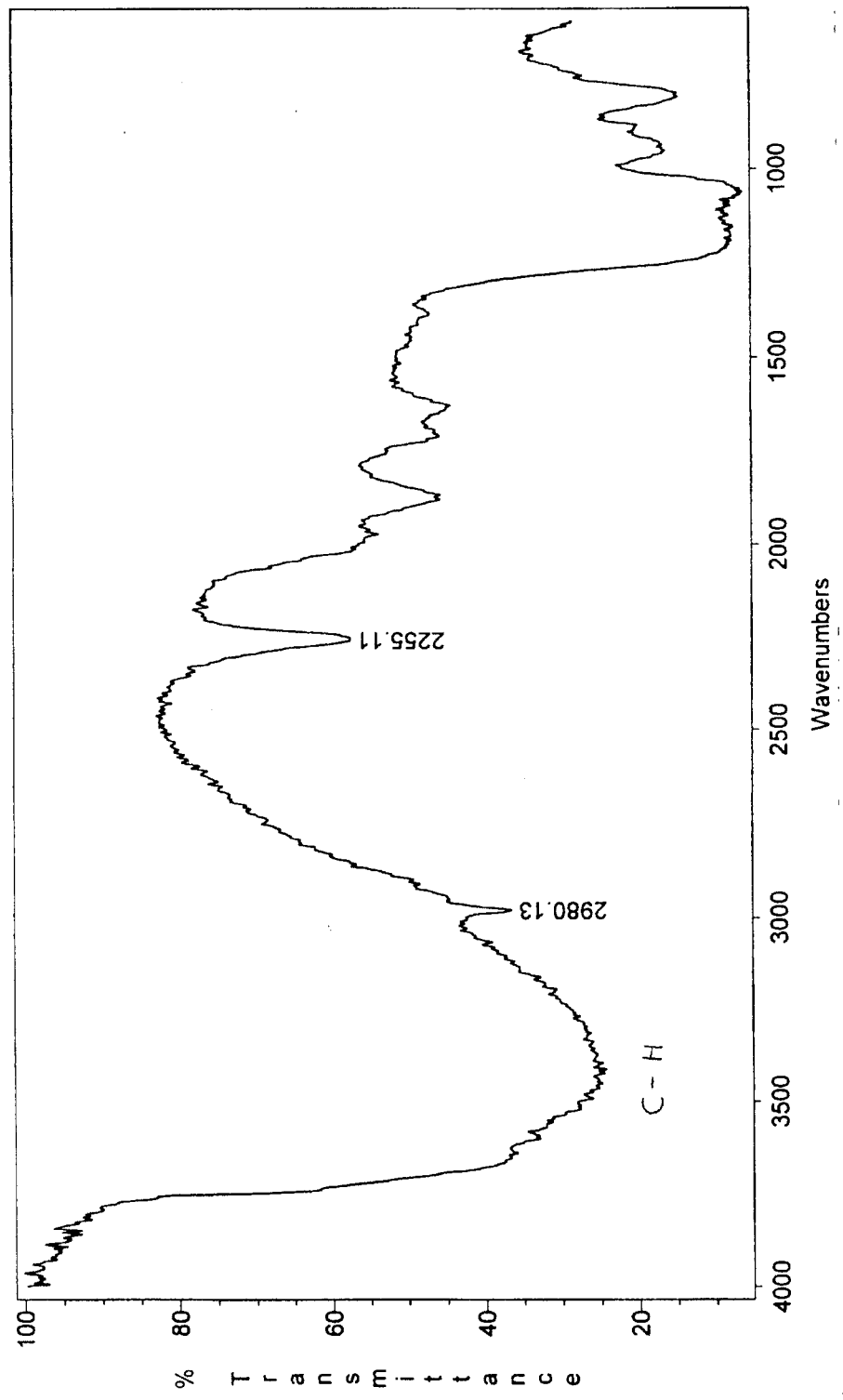
attached to the silica surface, the greater the surface coverage will be and better separation efficiencies are predicted. As mentioned earlier, the maximum amount of silanol groups that can be modified on the silica surface has been estimated to be approximately 8 μmol/m^2. According to Desert Analytics (Tucson, AZ), the percentage of carbon present on the quinine modified silica is 2.21%. α_R for quinine was calculated to be 4.88 μmol/m^2. Therefore, more than half of the silanol groups have quinine attached.

E. Chromatographic Measurements

The retention factor, or capacity factor (k'), can be empirically determined from the retention time of the solute, t_r, and the dead time of a reference solute, t_o. The reference solute is not retained by the stationary phase. The equation that relates these values is: $k' = (t_r - t_o)/t_o$. The retention factor cannot be negative. When the enantiomers of a solute are partitioned, k_1' and k_2' are used to designate the retention factors for the first and second enantiomers, respectively. The selectivity factor, or separation factor (α), represents the degree of separation of the enantiomers. The equation used to calculate α from k_1' and k_2' is: $\alpha = k_2'/k_1'$. The selectivity factor can be improved by altering certain parameters such as mobile phase composition, stationary phase, pH, and temperature.

Figure 15. ^{13}C CP-MAS NMR spectrum for solid sample quinine.

Figure 16. ^{13}C CP-MAS NMR spectrum for quinine bonded to Vydac silica hydride.
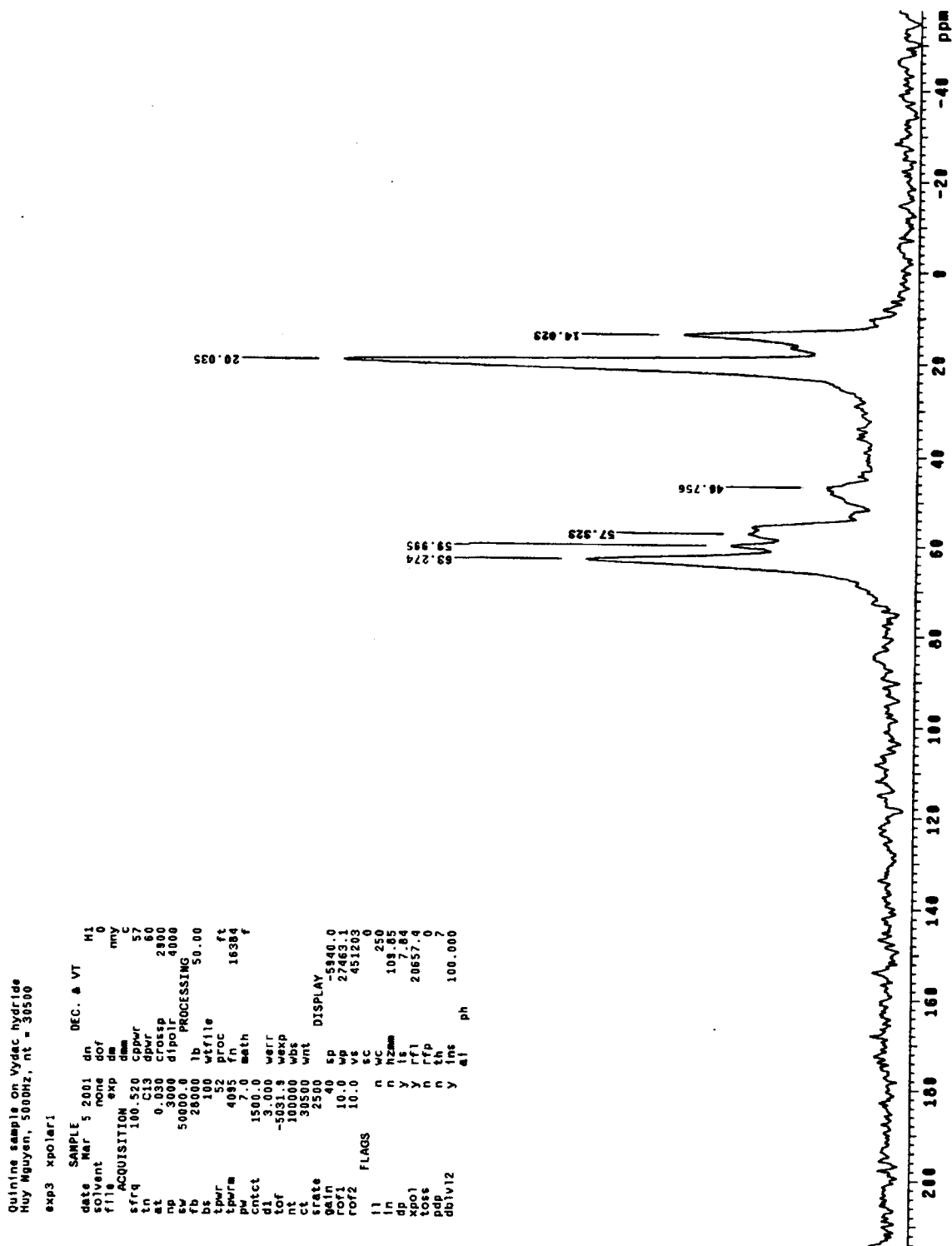
F. Solutes and Interpretation

The dead time of a reference solute, t_o, for all the following solutes are either 2 min or 1.6 min for flow rates of 0.5 mL/min and 0.4 mL/min, respectively. A high k' value means that the solute has a longer retention time. A high selectivity factor equates to greater separation of the enantiomers of a solute. The general goal of chiral separations is achieving low k' values while at the same time, achieving high α values. Methanol and acetonitrile are organic modifiers with respect to the substituted beta-cyclodextrin column because they compete with solutes for entering into the hydrophobic cavity. Substituted β-cyclodextrin CSP achieves separation mainly on inclusion complex formation; a hydrophobic cavity retains solutes by having favorable hydrophobic, non-polar interactions, and also by consisting of specific geometric configurations and sizes, only certain shapes and sizes of solutes may enter. In contrast, the quinine CSP achieves separation mainly by Pirkle-type interactions.

1. Binaphthol

The substituted β-cyclodextrin column had more success in separating (R)-binaphthol and (S)-binapthol than the quinine column. There were three successful separations using the β-cyclodextrin column in contrast to one separation using the quinine column. 40% acetonitrile resulted in greater k' values (1.03 and 1.19) for the substituted beta-cyclodextrin column than 90% and 80% acetonitrile. Since there is less acetonitrile, the binaphthol enantiomers are retained in the cavity longer. The cyclodextrin column consistently shows greater separation of binaphthol enantiomers by larger selectivity factors (e.g. 1.48) than the quinine column (e.g. 1.11). Tables 3-4 show the mobile phase

53

composition, t_r, k', and alpha parameters. Figures 17 - 18 are chromatograms in which separation was successful.

2. TFAE

The substituted β-cyclodextrin column had more success in separating (R)-TFAE and (S)-TFAE than the quinine column, as evident in Tables 5-6. As expected, 40% acetonitrile resulted in greater k' values (1.09 and 1.20) for the enantiomers than 90% and 80% acetonitrile. In general, the greater selectivity factors (e.g. 1.44) using the substituted beta-cyclodextrin column demonstrates this CSP's better ability to resolve enantiomers of TFAE than quinine (e.g. 1.11). Figure 19 shows the structure of TFAE in one of the enantiomeric forms. Due to the presence of 5 chiral centers, 3 rings, and a hydroxyl group, Pirkle type interactions result in enantiomeric separation in the quinine column. Hydrophobic interactions between the hydrophobic cavity of beta-cyclodextrin and the 3 rings of TFAE contribute to separation. Figure 20 is a chromatogram in which separation was partially successful.

3. Antibiotics

Only the quinine column was able to separate the enantiomers of chlortetracycline. The beta-cyclodextrin column did not resolve the isomers of chlortetracycline; there was only one peak. Table 7 shows the mobile phase composition and separation parameters. Figure 21 shows the structure of chlortetracycline. Due to the presence of 1 chiral center, 4 rings, 5 hydroxyl groups, and a NH_2 group, Pirkle type interactions result in enantiomeric separation using the quinine column. The cyclodextrin column was

Table 3. Mobile phase composition and retention times for the substituted beta-cyclodextrin column using *R*-binaphthol and *S*-binaphthol as the solute.

mobile phase composition	tr (min)	k'	alpha
90% acetonitrile	3.23	0.62	
	3.82	0.91	1.48
80% acetonitrile	2.98	0.49	
	3.45	0.72	1.47
40% acetonitrile	4.06	1.03	
	4.38	1.19	1.16

Table 4. Mobile phase composition and retention times for the quinine column using *R*-binaphthol and *S*-binaphthol as the solute.

mobile phase composition	tr (min)	k'	alpha
60% methanol	4.10	1.05	
	4.33	1.16	1.11

Figure 17. Separation of enantiomers of binaphthols (substituted β-cyclodextrin column; mobile phase - 80% acetonitrile:20% water; flow rate = 0.5 mL/min; temperature = 25°C; λ = 254 nm; injection volume = 20 μL).
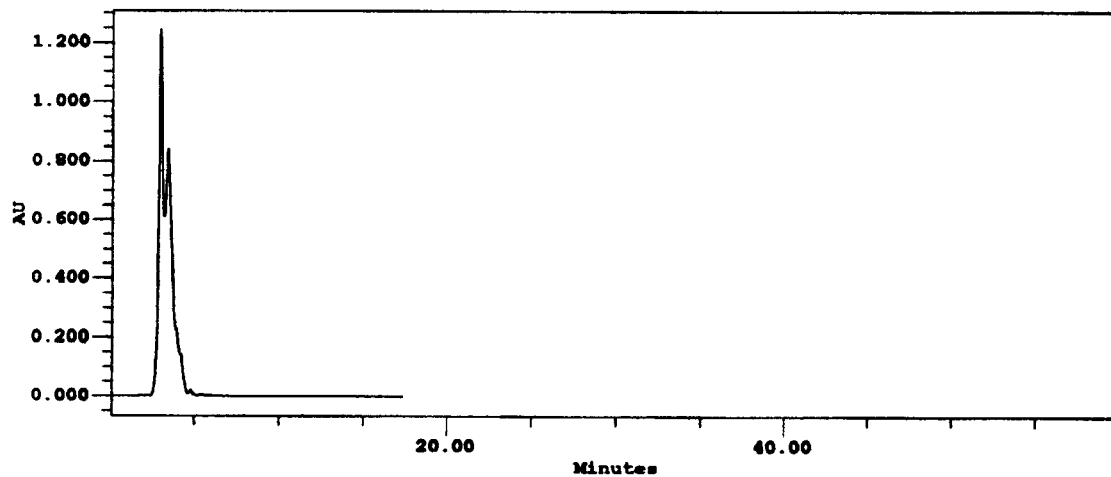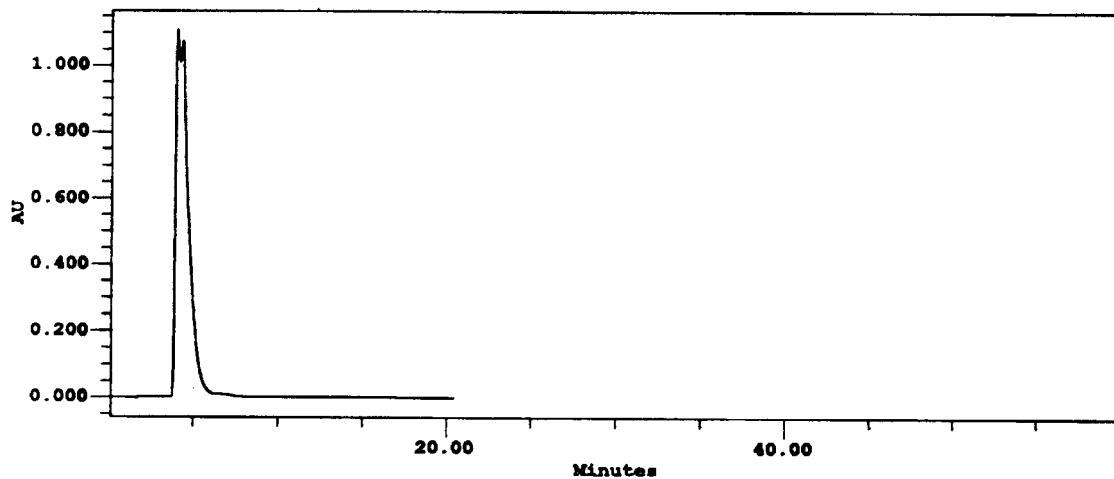
Figure 18. Separation of enantiomers of binaphthols (substituted β-cyclodextrin column; mobile phase - 40% acetonitrile:60% water; flow rate = 0.5 mL/min; temperature = 25°C; λ = 254 nm; injection volume = 20 μL).

unable to separate the chlortetracycline enantiomers probably due to the large size of the solute.

The quinine column had more success in separating the enantiomers of tetracycline than the substituted β-cyclodextrin column as seen in tables 8-9. The enantiomers of this solute were retained the greatest using 80% acetonitrile with respect to the quinine column, as evident of k' values of 2.24 and 4.33. In general, quinine was able to resolve the tetracycline enatiomers better, based on the alpha values, than the substituted beta-cyclodextrin column. The quinine column, using 80% acetonitrile, resulted in an alpha value of 1.93, while the cyclodextrin column, using 80% acetonitrile, showed 1.42 as the alpha value. Figure 22 shows the structure of tetracycline. Due to the presence of 4 chiral centers, 4 rings, 5 hydroxyl groups, and a NH_2 group, Pirkle type interactions result in enantiomeric separation in the quinine column. It appears that R_1 plays a role in cyclodextrin's ability to separate. If R_1 = H, as with tetracycline, there is separation using the cyclodextrin column. If R_1 = Cl, which has a greater atomic radius than H, there is likely no separation. Figures 23 and 24 are chromatograms in which separation was successful.

4. Drugs

Only the quinine column was able to separate the enantiomers of clenbuterol, a steroid. Table 10 shows the mobile phase composition and separation parameters. Higher methanol percentage in the mobile phase resulted in greater k' values and alpha value.

58

Only the quinine column was able to separate the enantiomers of terbutaline, a bronchodilating drug. Table 11 shows the mobile phase composition and separation parameters. Figure 25 shows the structure of terbutaline. Due to the presence of 1 ring, 3 hydroxyl groups, and a NH group, Pirkle type interactions result in enantiomeric separation in the quinine column. The large substituent, consisting of the *t*-butyl group, may prevent the solute from entering the hydrophobic cavity of beta-cyclodextrin.

Only the substituted β-cyclodextrin column was able to separate the enantiomers of tropicamide, a dilating drug. 80% acetonitrile resulted in greater k' values, but showed a lower alpha than 60% acetonitrile. Hence, the enantiomers were retained longer, but not separated as well. Table 12 shows the mobile phase composition and separation parameters. Figure 26 shows the structure of tropicamide. Due to the presence of 2 rings in the solute, formation of inclusion complexes resulted in enantiomeric separation. Figure 27 is a chromatogram in which separation was successful.

There were no separations seen with imipramine, a tricyclic antidepressant, due to the lack of a chiral center despite the presence of 3 rings. Figure 28 shows the structure of imipramine.

Only the substituted β-cyclodextrin column was able to separate the enantiomers of nortriptyline, a tricyclic antidepressant. Table 13 shows the mobile phase composition and retention times. Figure 29 shows the structure of nortriptyline. Due to the presence of 3 rings, formation of inclusion complexes resulted in enantiomeric separation using the substituted beta-cyclodextrin column. Nortrityline does not have a chiral center.

Table 5. Mobile phase composition and retention times for the substituted beta-cyclodextrin column using R-TFAE and S-TFAE as the solute.

mobile phase composition	tr (min)	k'	alpha
90% acetonitrile	3.22	0.61	
	3.74	0.87	1.43
80% acetonitrile	2.95	0.48	
	3.37	0.69	1.44
40% acetonitrile	4.18	1.09	
	4.40	1.20	1.10

Table 6. Mobile phase composition and retention times for the quinine column using R-TFAE and S-TFAE as the solute.

mobile phase composition	tr (min)	k'	alpha
60% methanol	4.11	1.06	
	4.34	1.17	1.11

Figure 19. Structure of (*R*)-(-)-2,2,2-trifluoro-1-(9-anthryl) ethanol.
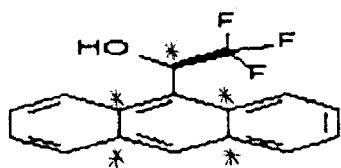
Figure 20. Separation of enantiomers of TFAE (substituted β-cyclodextrin column; mobile phase - 90% acetonitrile:10% water; flow rate = 0.5 mL/min; temperature = 25°C; λ = 254 nm; injection volume = 20 μL).
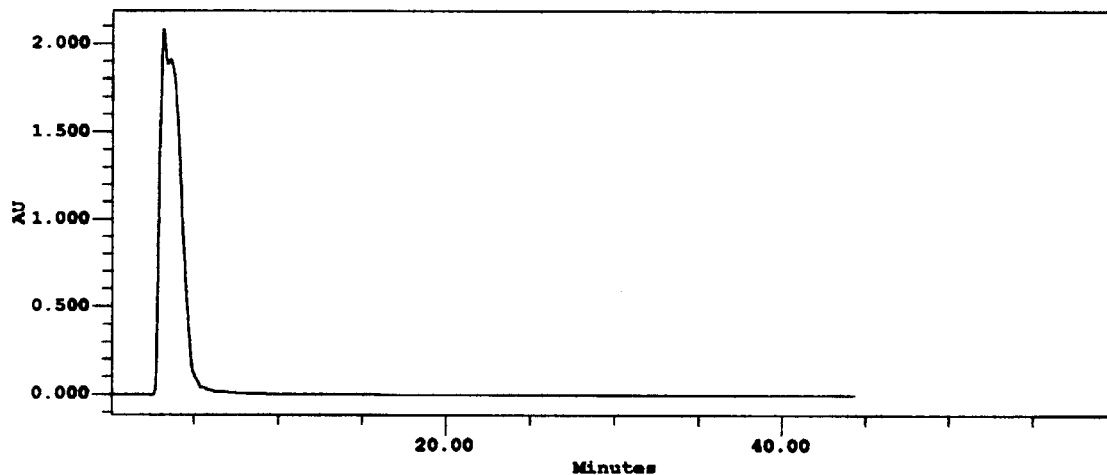
Table 7. Mobile phase composition and retention times for the quinine column using chlortetracycline as the solute.

mobile phase composition	tr (min)	k'	alpha
90% methanol	3.45	0.73	
	4.63	1.32	1.81

Figure 21. Structure of chlortetracycline.
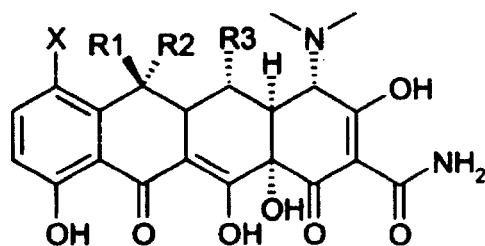
Name	X	R1	R2	R3
Tetracycline	H	OH	Me	H
Chlortetracycline	Cl	OH	Me	H
Oxytetracycline	H	OH	Me	OH
Demeclocycline	Cl	OH	H	H
Doxycycline	H	H	Me	OH
Minocycline	NMe_2	H	H	H
Methacycline	H	$=CH_2$	$=CH_2$	OH

Table 8. Mobile phase composition and retention times for the substituted beta-cyclodextrin column using tetracycline as the solute.

mobile phase composition	tr (min)	k'	alpha
80% acetonitrile	7.86	2.93	
	10.31	4.15	1.42

Table 9. Mobile phase composition and retention times for the quinine column using tetracycline as the solute.

mobile phase composition	tr (min)	k'	alpha
90% acetonitrile	4.61	1.30	
	6.02	2.01	1.54
80% acetonitrile	6.48	2.24	
	10.66	4.33	1.93
60% acetonitrile	5.12	1.56	
	6.81	2.41	1.54
40% acetonitrile	5.80	1.90	
	5.90	1.95	1.03

Figure 22. Structure of tetracycline.

Figure 23. Separation of enantiomers of tetracycline (substituted β-cyclodextrin column; mobile phase - 80% acetonitrile:20% water; flow rate = 0.5 mL/min; temperature = 25°C; λ = 254 nm; injection volume = 20 μL).
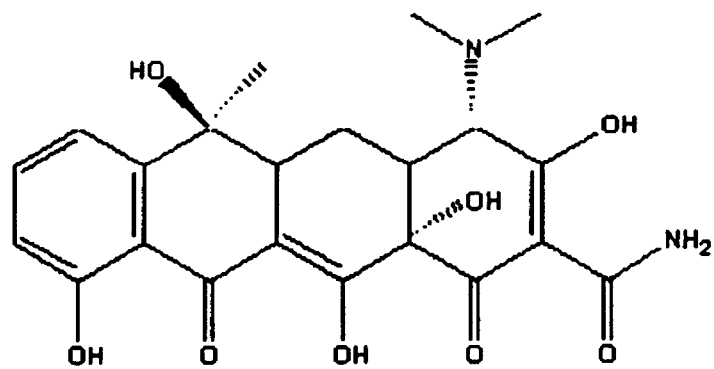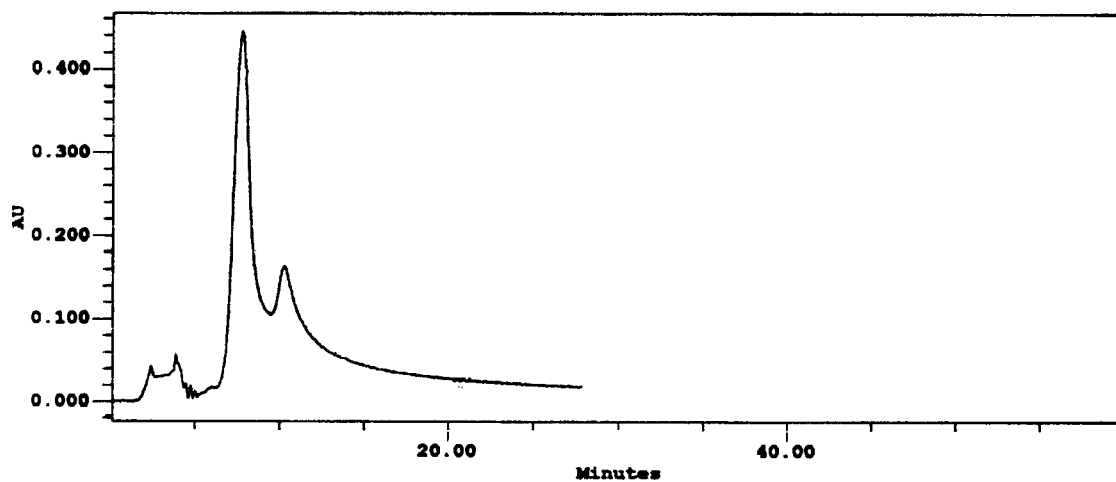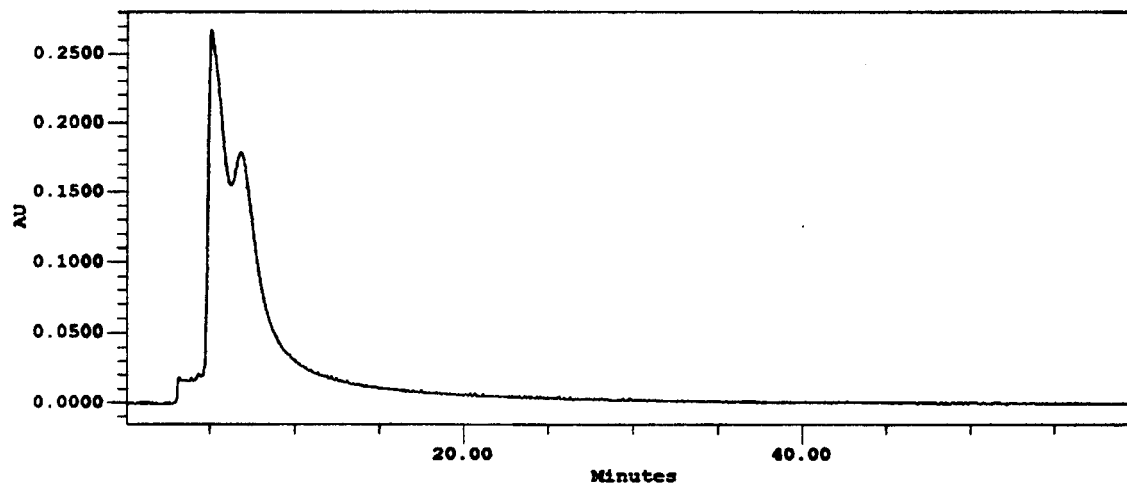

67

Figure 24. Separation of enantiomers of tetracycline (quinine column; mobile phase - 60% acetonitrile:40% water; flow rate = 0.5 mL/min; temperature = 25°C; λ = 254 nm; injection volume = 20 μL).

The substituted β-cyclodextrin column had more success in separating the enantiomers of

oxazepam, a benzodiazepine, than the quinine column with five separations as shown in tables

14-15. Although the separation of enantiomers, represented by similar alpha values, using both

columns were similar, the substituted beta-cyclodextrin column showed greater retention of the

solutes, as shown by high k' values. Figure 30 shows the structure of oxazepam. Due to the

presence of 1 chiral center, 3 rings, 1 hydroxyl group, and 1 NH group, Pirkle type interactions

result in enantiomeric separation using the quinine column. The existence of three rings and

the compactness of the solute favors formation of inclusion complexes with the beta-

cyclodextrin. Figures 31-32 are chromatograms of successful separations.

Only the temazepam, a benzodiazepine as shown in table 16. 40% methanol resulted in the

greatest k' values of 3.51 and 3.90, while 90% acetonitrile showed the greatest selectivity

factor of 1.23. Figure 33 shows the structure of temazepam. Due to the presence of 3 rings, an

inclusion complex may have formed between the beta-cyclodextrin CSP and the solute.

Figures 34-35 are chromatograms of successful separation.

5. DL-homatropine

Only the quinine column was able to separate the enantiomers of DL-homatropine. Table

17 shows the mobile phase composition and separation parameters. 60% methanol and 40%

methanol showed similar retention factors; however, 60% methanol resulted in a greater alpha

value of 1.22, in contrast to 1.08. Figure 36 shows the structure of DL-homatropine. Due to

the presence of 4 chiral centers, 2 rings, and 1 hydroxyl group, Pirkle type interactions result in

enantiomeric separation using the quinine column. The large size of DL-homatropine may

prevent formation of inclusion complexes.

Table 10. Mobile phase composition and retention times for the quinine column using clenbuterol as the solute.

mobile phase composition	tr (min)	k'	alpha
80% methanol	20.91	9.45	
	34.35	16.18	1.71
40% methanol	3.94	0.97	
	4.15	1.07	1.11

Table 11. Mobile phase composition and retention times for the quinine column using terbutaline as the solute.

mobile phase composition	tr (min)	k'	alpha
60% methanol	3.09	0.55	
	4.35	1.18	2.16

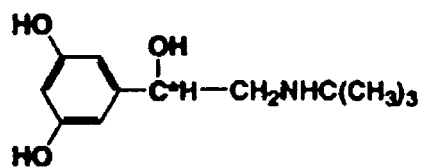Figure 25. Structure of terbutaline.

Table 12. Mobile phase composition and retention times for the substituted beta-cyclodextrin column using tropicamide as the solute.

mobile phase composition	tr (min)	k'	alpha
80% acetonitrile	4.55	1.28	
	4.96	1.48	1.16
60% acetonitrile	3.79	0.89	
	4.16	1.08	1.21

Figure 26. Structure of tropicamide.
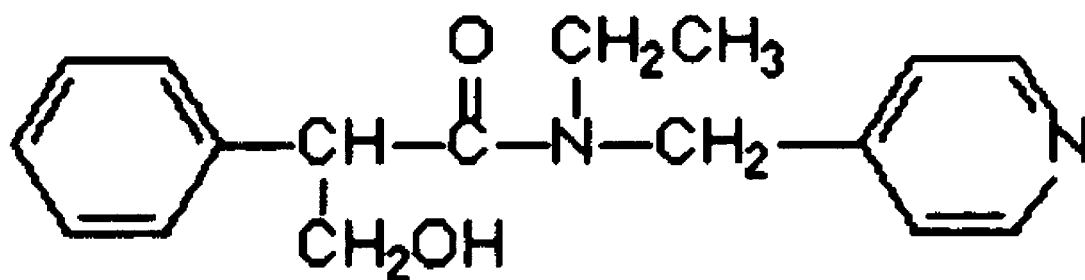
Figure 27. Separation of enantiomers of tropicamide (substituted β-cyclodextrin column; mobile phase - 60% acetonitrile:40% water; flow rate = 0.5 mL/min; temperature = 25°C; λ = 254 nm; injection volume = 20 μL).

Figure 28. Structure of imipramine.

Table 13. Mobile phase composition and retention times for the substituted beta-cyclodextrin column using nortriptyline as the solute.

mobile phase composition	tr (min)	k'	alpha
60% acetonitrile	2.27	0.14	
	3.59	0.80	5.86

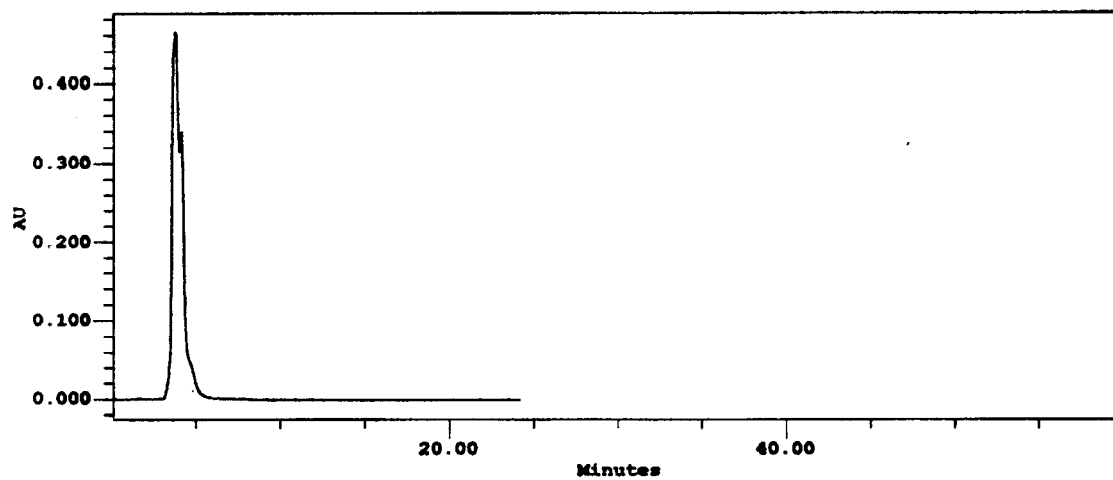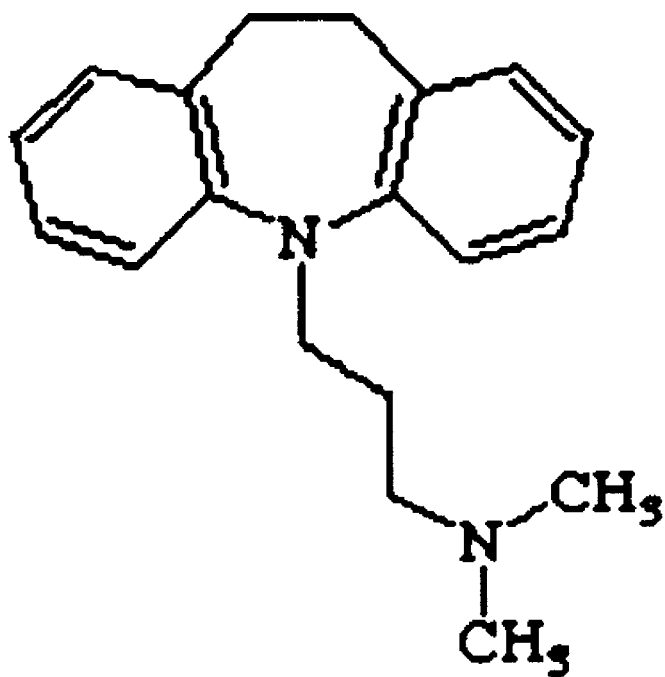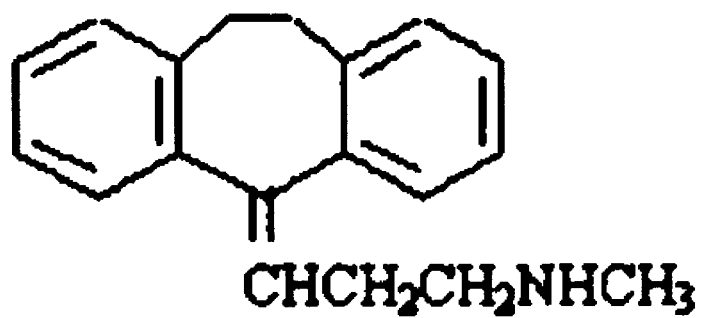Figure 29. Structure of nortriptyline.

$CHCH_2CH_2NHCH_3$

6. 2-phenoxypropionic Acid

The substituted β-cyclodextrin column had less success in separating the enantiomers of 2-phenoxypropionic acid than the quinine column as shown in tables 18-19. In general, the selectivity factors afforded by the quinine column was better than the cyclodextrin column. Figure 37 shows the structure of 2-phenoxypropionic acid. Due to the presence of 1 chiral center, 1 ring, and 1 hydroxyl group, Pirkle type interactions result in enantiomeric separation on the quinine column. Figure 38 is a chromatogram showing a successful separation.

7. Alcohols

The substituted β-cyclodextrin column had four successful separations of the 2-phenyl-1,2-propanediol enantiomers, in contrast to one successful separation achieved by the quinine column. Tables 20-21 show the mobile phase composition and separation parameters. Better separation of the enantiomers were seen using the substituted beta-cyclodextrin column, as evidenced by higher alpha values. Additionally, the solute was retained longer on the cyclodextrin column; the smallest k' value was 6.93 minutes, in contrast to 1.18 min on the quinine column. Figures 39-41 are chromatograms showing successful separations.

Both columns had equal success in separating the enantiomers of 1-phenyl-2-propanol, each with one successful separation, as shown in tables 22-23. The alpha and k' values for both columns were quite similar. Figure 42 shows the structure of 1-phenyl-2-propanol. Due to the presence of 1 chiral center, 1 ring, and 1 hydroxyl group, Pirkle type interactions result in enantiomeric separation on the quinine column. Also, the ring

Table 14. Mobile phase composition and retention times for the substituted beta-cyclodextrin column using oxazepam as the solute.

mobile phase composition	tr (min)	k'	alpha
60% methanol	5.64	2.52	
	6.31	2.95	1.17
50% methanol	6.09	2.81	
	7.30	3.56	1.27
40% methanol	7.80	3.87	
	10.84	5.78	1.49
90% acetonitrile	3.95	0.97	
	4.24	1.12	1.15
80% acetonitrile	3.74	0.87	
	4.25	1.13	1.29

Table 15. Mobile phase composition and retention times for the quinine column using oxazepam as the solute.

mobile phase composition	tr (min)	k'	alpha
90% methanol	4.15	1.07	
	4.62	1.31	1.22

Figure 30. Structure of oxazepam.

Figure 31. Separation of enantiomers of oxazepam (substituted β-cyclodextrin column; mobile phase - 60% methanol:40% water; flow rate = 0.4 mL/min; temperature = 25°C; λ = 254 nm; injection volume = 4 μL).
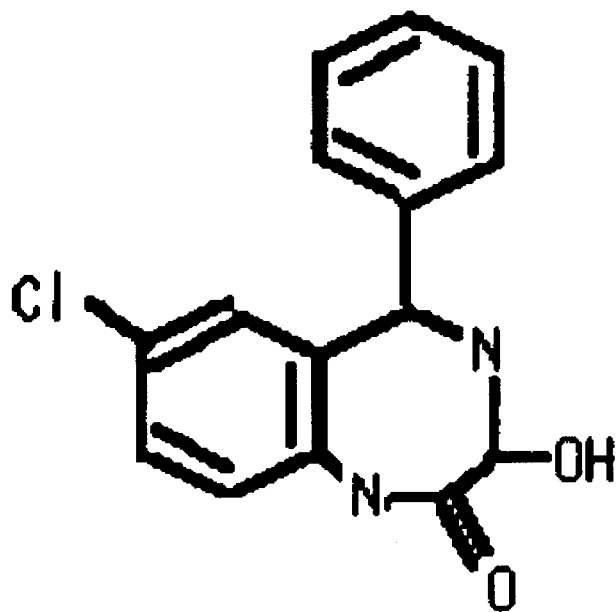
Figure 32. Separation of enantiomers of oxazepam (substituted β-cyclodextrin column; mobile phase - 50% methanol:50% water; flow rate = 0.4 mL/min; temperature = 25°C; λ = 254 nm; injection volume = 4 μL).
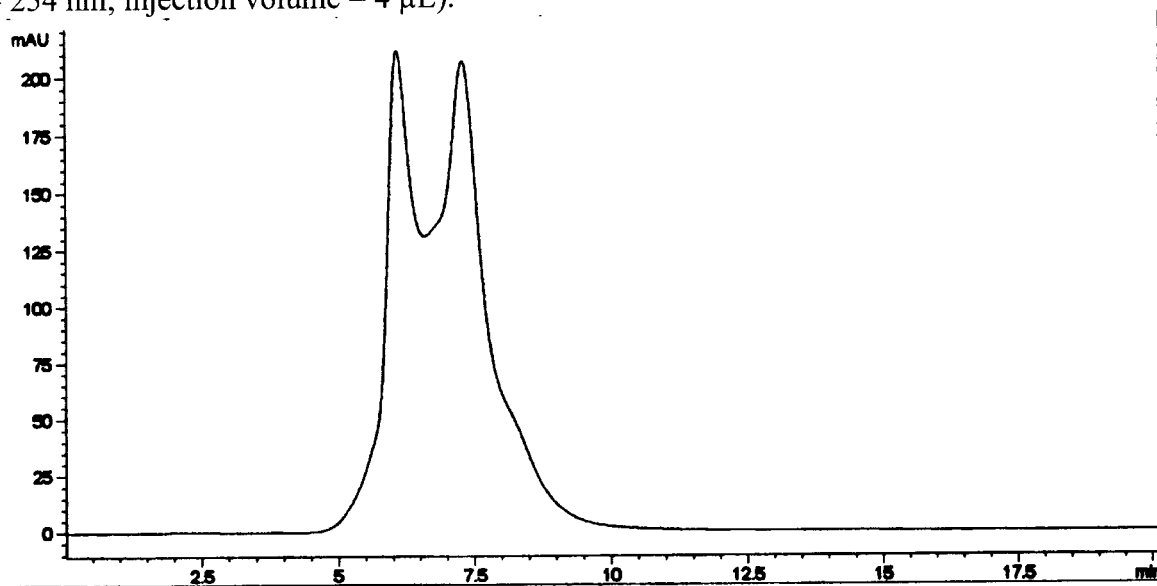
Table 16. Mobile phase composition and retention times for the substituted beta-cyclodextrin column using temazepam as the solute.

mobile phase composition	tr (min)	k'	alpha
40% methanol	7.21	3.51	
	7.83	3.90	1.11
90% acetonitrile	3.74	0.87	
	4.14	1.07	1.23
80% acetonitrile	3.35	0.67	
	3.61	0.80	1.19

Figure 33. Structure of temazepam.

Figure 34. Separation of enantiomers of temazepam (substituted β-cyclodextrin column; mobile phase - 40% methanol:60% water; flow rate = 0.4 mL/min; temperature = 25°C; λ = 254 nm; injection volume = 4 μL).
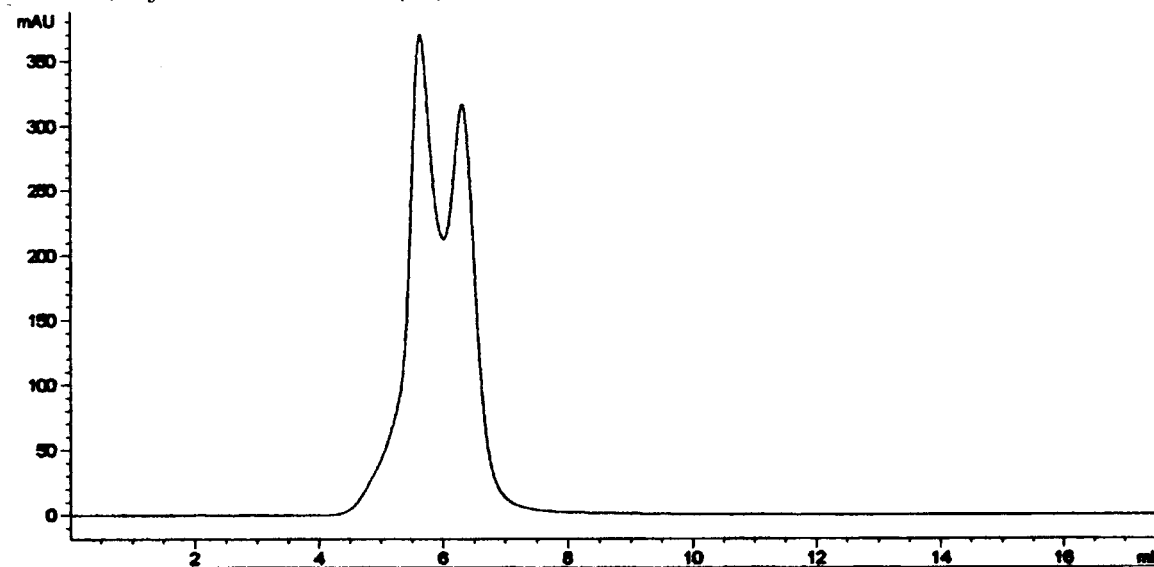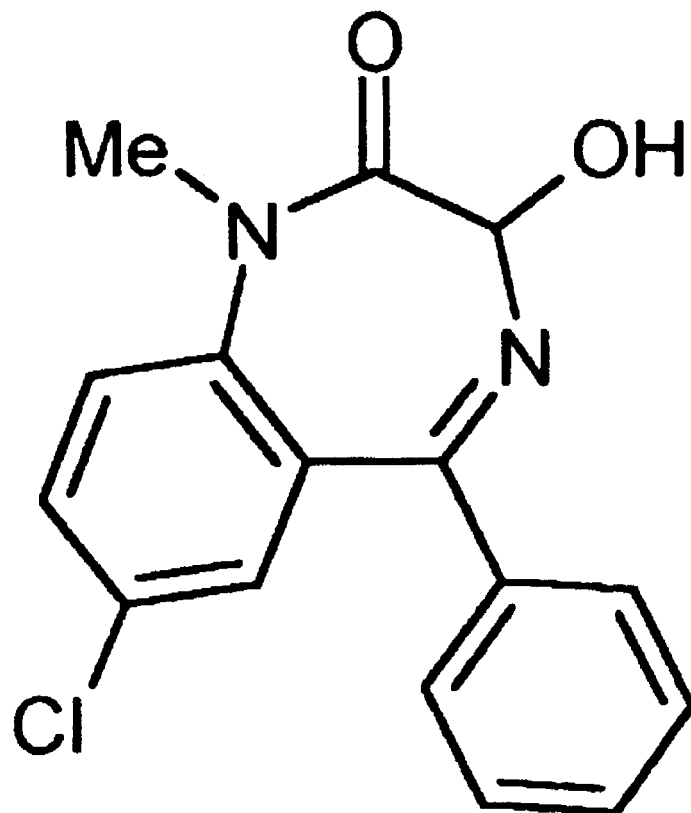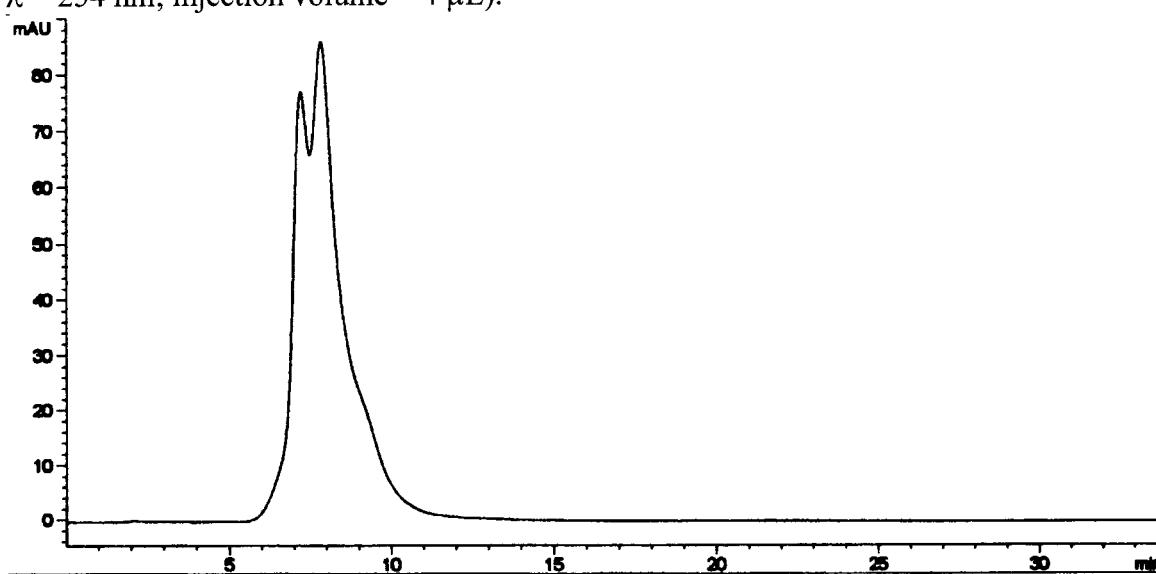
Figure 35. Separation of enantiomers of temazepam (substituted β-cyclodextrin column; mobile phase - 90% acetonitrile:10% water; flow rate = 0.5 mL/min; temperature = 25°C; λ = 254 nm; injection volume = 20 μL).

Table 17. Mobile phase composition and retention times for the quinine
column using DL-homatropine as the solute.

mobile phase composition	tr (min)	k'	alpha
60% methanol	3.89	0.95	
	4.30	1.15	1.22
40% methanol	3.95	0.98	
	4.10	1.05	1.08

Figure 36. Structure of DL-homatropine.

may have favored hydrophobic interactions with the hydrophobic cavity of the cyclodextrin column.

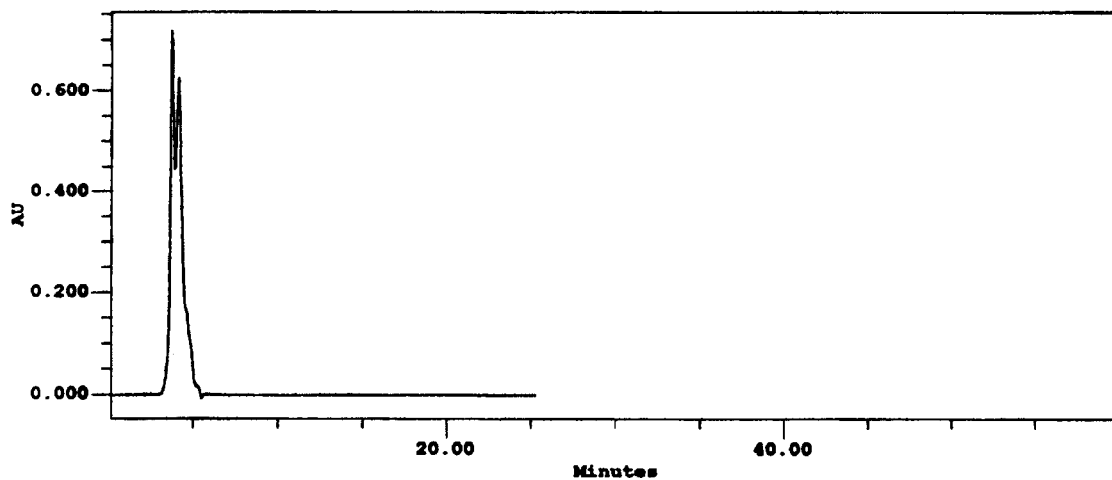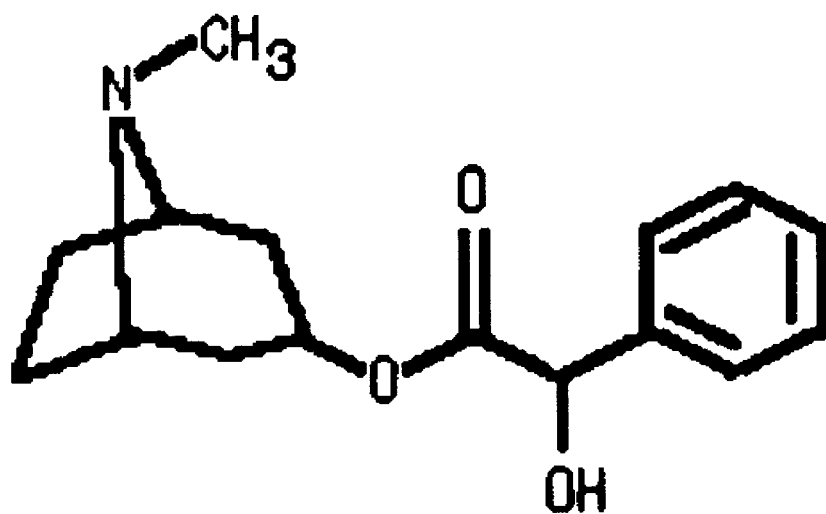Only the substituted β-cyclodextrin column was successful in separating the enantiomers of DL-propranolol. Table 24 shows the mobile phase composition and separation parameters. The peaks representing the enantiomers were greatly resolved, as evident of the high alpha value of 11.83. Figure 43 shows the structure of DL-propranolol. Due to the presence of 2 rings, formation of an inclusion complex resulted in enantiomeric separation.

8. $[Ru(bipy)_3]^{2+}$

The substituted β-cyclodextrin column had 3 successful separations of the enantiomers of $[Ru(bipy)_3]^{2+}$ while the quinine column only had 2 successful separations. Tables 25-26 show the mobile phase composition and separation parameters. 40% acetonitrile resulted in the best separation of the enantiomers due to an alpha value of 2.06. On the other hand, 40% methanol retained the solutes longer; the k' values were 1.75 and 2.00 min for the enantiomers, respectively. Figures 44-46 are chromatograms of successful separations.

9. Novel Selenium Compounds

All Selenium compounds were synthesized in the laboratory of Dr. Brenda Kesler. Figure 47 shows the structure of SW-II-69B. The substituted β-cyclodextrin column had more success in separating the enantiomers of SW-II-69B than the quinine column as shown in tables 27-28. Overall, the beta-cyclodextrin column resolved the enantiomeric

Table 18. Mobile phase composition and retention times for the substituted beta-cyclodextrin column using 2-phenoxypropionic acid as the solute.

mobile phase composition	tr (min)	k'	alpha
40% acetonitrile	3.75	0.88	
	4.11	1.05	1.20

Table 19. Mobile phase composition and retention times for the quinine column using 2-phenoxypropionic acid as the solute.

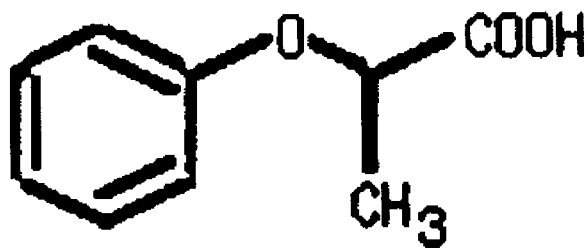| mobile phase composition	tr (min)	k'	alpha
40% methanol	3.97	0.99	
	4.34	1.17	1.19
90% acetonitrile	4.48	1.24	
	5.20	1.60	1.29
60% acetonitrile	3.51	0.76	
	4.14	1.07	1.41
40% acetonitrile	3.81	0.90	
	4.27	1.14	1.26

Figure 37. Structure of 2-phenoxypropionic acid.

Figure 38. Separation of enantiomers of 2-phenoxypropionic acid (substituted β-cyclodextrin column; mobile phase - 40% acetonitrile:60% water; flow rate = 0.5 mL/min; temperature = 25°C; λ = 254 nm; injection volume = 20 μL).
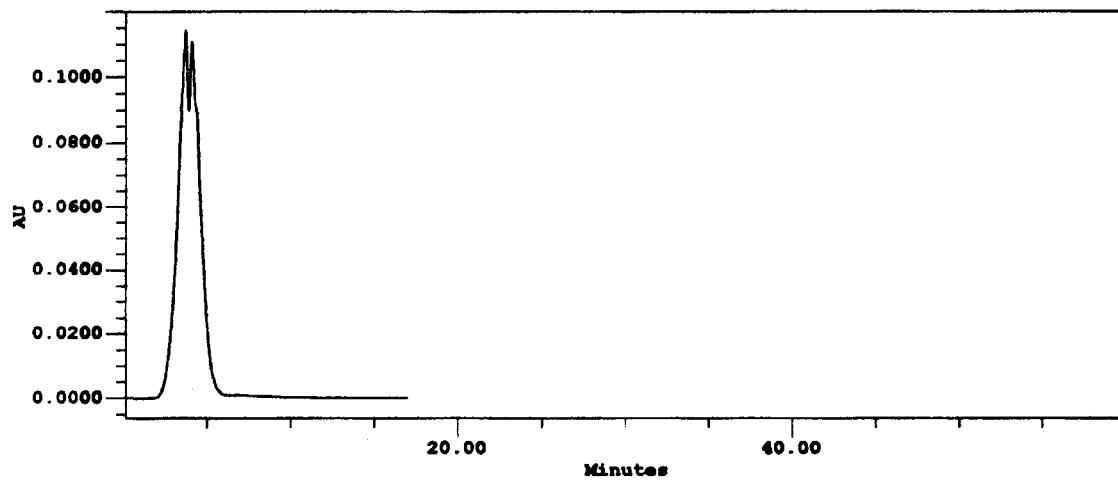
Table 20. Mobile phase composition and retention times for the substituted beta-cyclodextrin column using 2-phenyl-1,2-propanediol as the solute.

mobile phase composition	tr (min)	k'	alpha
70% methanol	33.14	15.57	
	37.04	17.52	1.13
60% methanol	61.75	29.88	
	78.38	38.19	1.28
50% methanol	6.93	3.33	
	9.81	5.13	1.54
40% methanol	8.63	4.40	
	9.73	5.08	1.16

Table 21. Mobile phase composition and retention times for the quinine column using 2-phenyl-1,2-propanediol as the solute.

mobile phase composition	tr (min)	k'	alpha
90% methanol	4.17	1.08	
	4.36	1.18	1.09

Figure 39. Separation of enantiomers of 2-phenyl-1,2-propanediol (substituted β-cyclodextrin column; mobile phase - 70% methanol:30% water; flow rate = 0.5 mL/min; temperature = 25°C; λ = 254 nm; injection volume = 4 µL).

Figure 40. Separation of enantiomers of 2-phenyl-1,2-propanediol (substituted β-cyclodextrin column; mobile phase - 60% methanol:40% water; flow rate = 0.5 mL/min; temperature = 25°C; λ = 254 nm; injection volume = 4 μL).
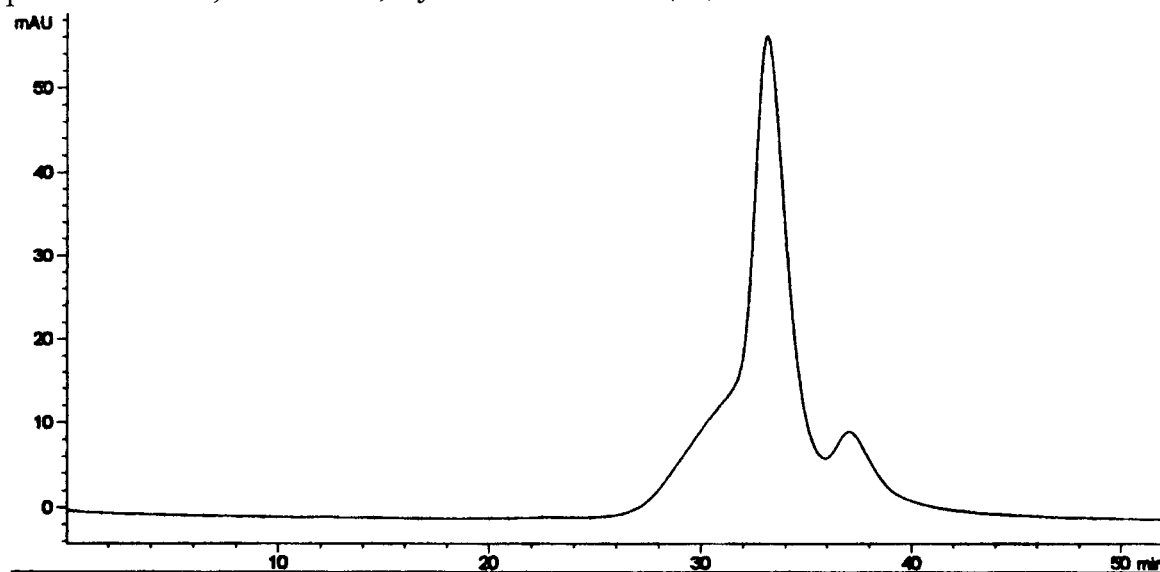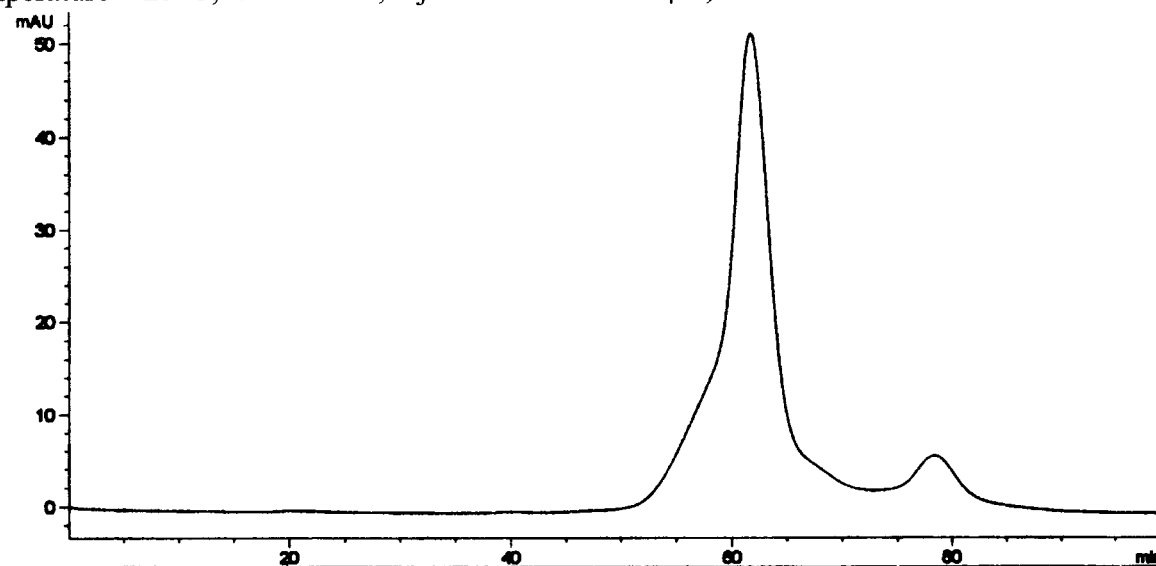
Figure 41. Separation of enantiomers of 2-phenyl-1,2-propanediol (substituted β-cyclodextrin column; mobile phase - 40% methanol:60% water; flow rate = 0.4 mL/min; temperature = 25°C; λ = 254 nm; injection volume = 4 μL).

Table 22. Mobile phase composition and retention times for the substituted beta-cyclodextrin column using 1-phenyl-2-propanol as the solute.

mobile phase composition	tr (min)	k'	alpha
90% acetonitrile	4.45	1.23	
	4.74	1.37	1.12

Table 23. Mobile phase composition and retention times for the quinine column using 1-phenyl-2-propanol as the solute.

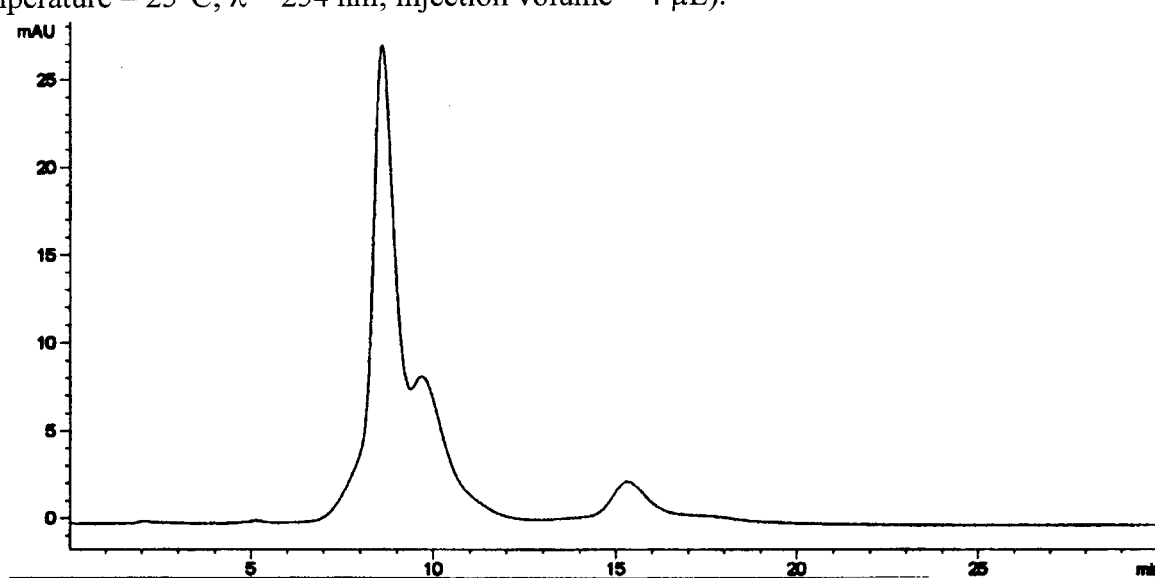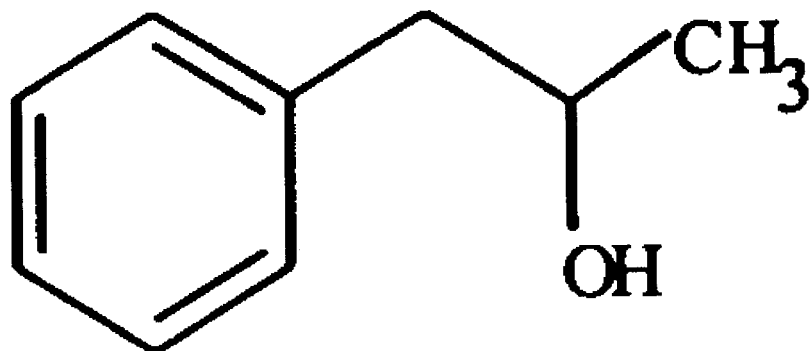| mobile phase composition	tr (min)	k'	alpha
80% methanol	4.10	1.05	
	4.37	1.19	1.13

Figure 42. Structure of 1-phenyl-2-propanol.

Table 24. Mobile phase composition and retention times for the substituted beta-cyclodextrin column using DL-propranolol as the solute.

mobile phase composition	tr (min)	k'	alpha
60% acetonitrile	2.13	0.07	
	3.59	0.79	11.83

Figure 43. Structure of DL-propranolol.
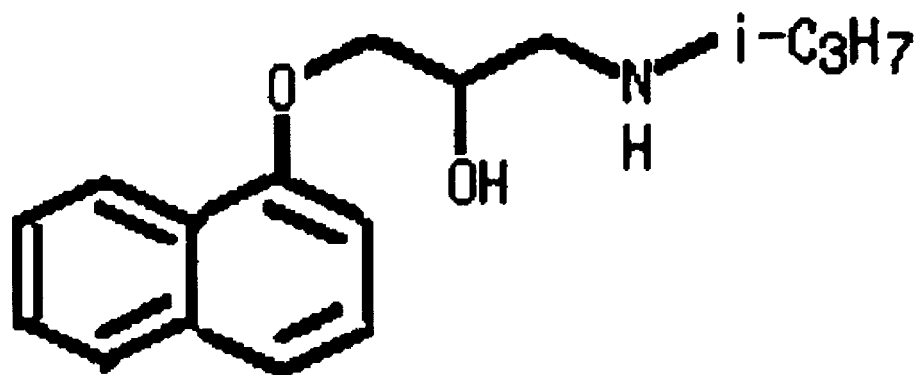
peaks better than the quinine column using alpha as the resolving parameter. Also, the

SW-II-69B enantiomers were retained longer on the cyclodextrin column. Due to the

presence of 1 chiral center and 2 rings, Pirkle type interactions result in enantiomeric

separation on the quinine column, while the 2 rings may contribute to inclusion complex

formation with the hydrophobic cavity of the cyclodextrin. Figures 48-50 are

chromatograms showing successful separations.

Figure 51 shows the structure of SW-II-71B. The substituted β-cyclodextrin column

had much more success in separating the enantiomers of SW-II-71B than the quinine

column; tables 29-30 show that the cyclodextrin column was able to separate the

enantiomers using five different solvents, while the quinine column was only able to

partition under one solvent condition. Using 60% methanol, the solute enantiomers were

highly resolved as shown with a selectivity factor vale of 2.98. Due to the presence of 1

chiral center and 2 rings, Pirkle type interactions result in enantiomeric separation on the

quinine column; the 2 rings may be involved in inclusion complex formation. Figure 52

is a chromatogram showing a successful separation.

The substituted β-cyclodextrin column had one more successful separation than

the quinine column in separating the enantiomers of SW-II-73B-OH. Tables 31-32

show that the enantiomeric peaks were resolved better than the quinine column; alpha

values of 1.13 and 1.18, for the beta-cyclodextrin column, is greater than the alpha

value of 1.09 for the quinine. Figure 53 shows the structure of SW-II-73B-OH. Due

to the presence of 1 chiral center, 2 rings, and 1 hydroxyl group, Pirkle type

interactions result in enantiomeric separation on the quinine column, while the 2 rings

contribute to inclusion complex formation with the hydrophobic cavity of the cyclodextrin column. Figures 54-55 are chromatograms showing successful separations.

The substituted β-cyclodextrin column had much more successful separation of the enantiomers of SW-II-75B-OCH$_3$ than the quinine column. Tables 33-34 shows the mobile phase composition and separation parameters. Regardless of the percentage of methanol or acetonitrile, the cyclodextrin column was able to resolve the peaks better than the quinine column. Figure 56 shows the structure of SW-II-75B-OCH$_3$. Due to the presence of 1 chiral center and 2 rings, Pirkle type interactions result in enantiomeric separation on the quinine column. Inclusion complex formation may occur due to the presence of 2 rings on SW-II-75B-OCH$_3$. Figures 57-59 are chromatograms showing successful separations.

The substituted β-cyclodextrin column had 5 successful separations of the enantiomers of SW-II-79B; the quinine column only had 2. Tables 35-36 show the that the selectivity factors were consistently higher for the cyclodextrin column. Figure 60 shows the structure of SW-II-79B. The aromatic ring on the solute may contribute to the formation of inclusion complexes, resulting in separation on the cyclodextrin column. Due to the presence of 1 chiral center and 1 ring, Pirkle type interactions result in enantiomeric separation on the quinine column. Figures 61-62 are chromatograms showing successful separations.

The substituted β-cyclodextrin column had 2 more success in separating the

Table 25. Mobile phase composition and retention times for the substituted beta-cyclodextrin column using $[Ru(bipy)_3]^{2+}$ as the solute.

mobile phase composition	tr (min)	k'	alpha
40% methanol	4.39	1.75	
	4.80	2.00	1.15
80% acetonitrile	3.77	0.88	
	4.76	1.38	1.56
40% acetonitrile	3.25	0.63	
	4.58	1.29	2.06

Table 26. Mobile phase composition and retention times for the quinine column using $[Ru(bipy)_3]^{2+}$ as the solute.

mobile phase composition	tr (min)	k'	alpha
60% methanol	4.31	1.16	
	5.83	1.91	1.65
40% methanol	4.36	1.18	
	5.84	1.92	1.63

Figure 44. Separation of enantiomers of $[Ru(bipy)_3]^{2+}$ (substituted β-cyclodextrin column; mobile phase - 40% methanol:60% water; flow rate = 0.4 mL/min; temperature = 25°C; λ = 280 nm; injection volume = 4 μL).
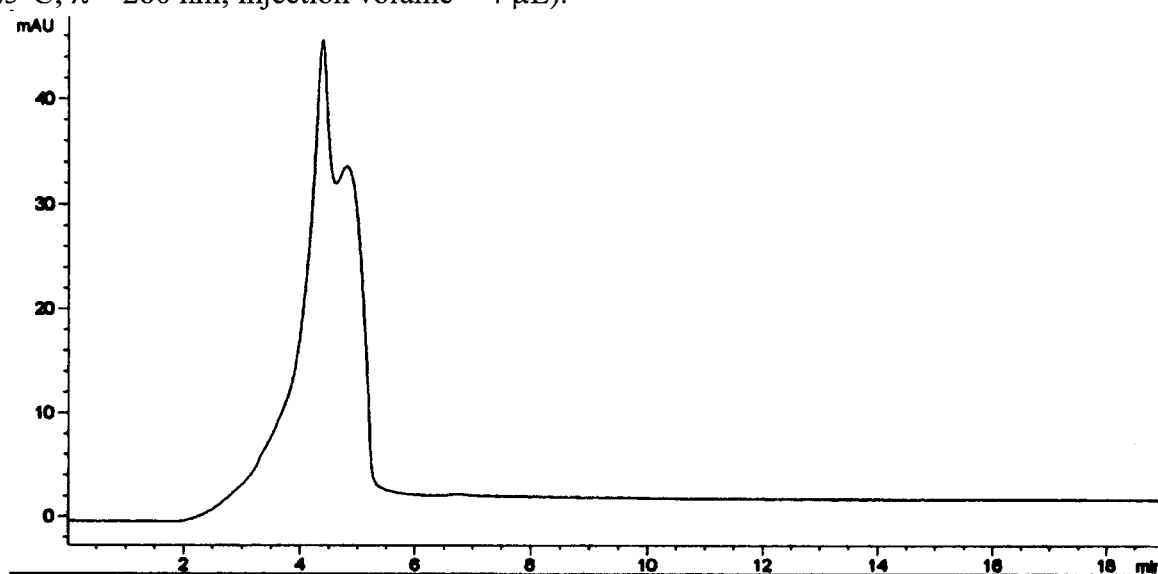
Figure 45. Separation of enantiomers of $[Ru(bipy)_3]^{2+}$ (substituted β-cyclodextrin column; mobile phase - 80% acetonitrile:20% water; flow rate = 0.5 mL/min; temperature = 25°C; λ = 280 nm; injection volume = 20 μL).
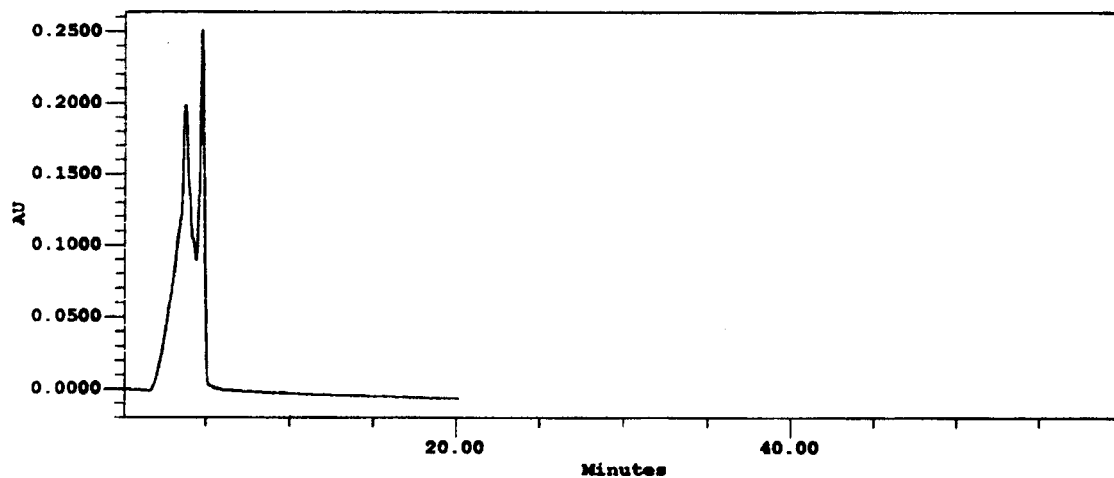
Figure 46. Separation of enantiomers of $[Ru(bipy)_3]^{2+}$ (substituted quinine column; mobile phase - 60% methanol:40% water; flow rate = 0.5 mL/min; temperature = 25°C; λ = 280 nm; injection volume = 20 μL).
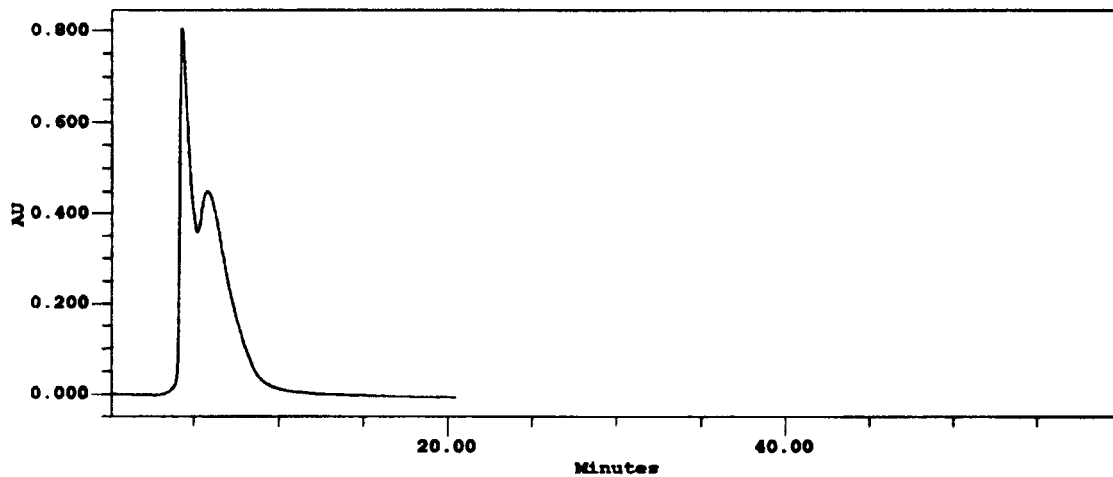
Table 27. Mobile phase composition and retention times for the substituted beta-cyclodextrin column using SW-II-69B as the solute.

mobile phase composition	tr (min)	k'	alpha
70% methanol	37.89	17.95	
	42.16	20.08	1.12
60% methanol	21.09	9.55	
	56.23	27.11	2.84
40% methanol	8.80	4.50	
	10.12	5.33	1.18
40% acetonitrile	4.77	1.39	
	6.28	2.14	1.55

Table 28. Mobile phase composition and retention times for the quinine column using SW-II-69B as the solute.

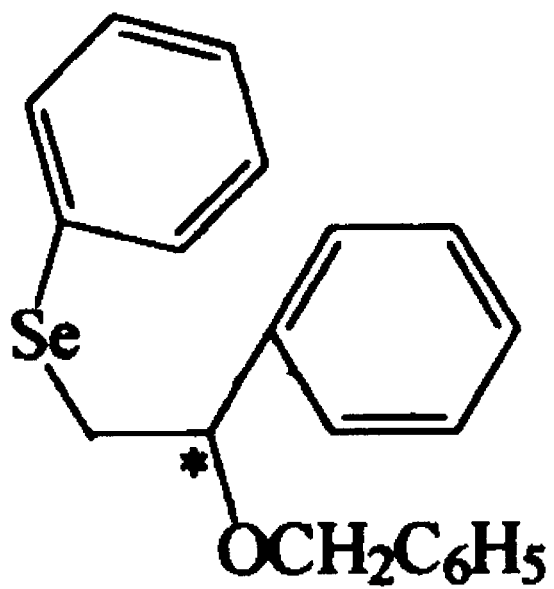| mobile phase composition	tr (min)	k'	alpha
80% methanol	4.11	1.05	
	4.34	1.17	1.11
80% acetonitrile	4.40	1.20	
	4.47	1.23	1.03

Figure 47. Structure of SW-II-69B.

OCH₂C₆H₅

Figure 48. Separation of enantiomers of SW-II-69B (substituted β-cyclodextrin column; mobile phase - 70% methanol:30% water; flow rate = 0.5 mL/min; temperature = 25°C; λ = 254 nm; injection volume = 4 μL).
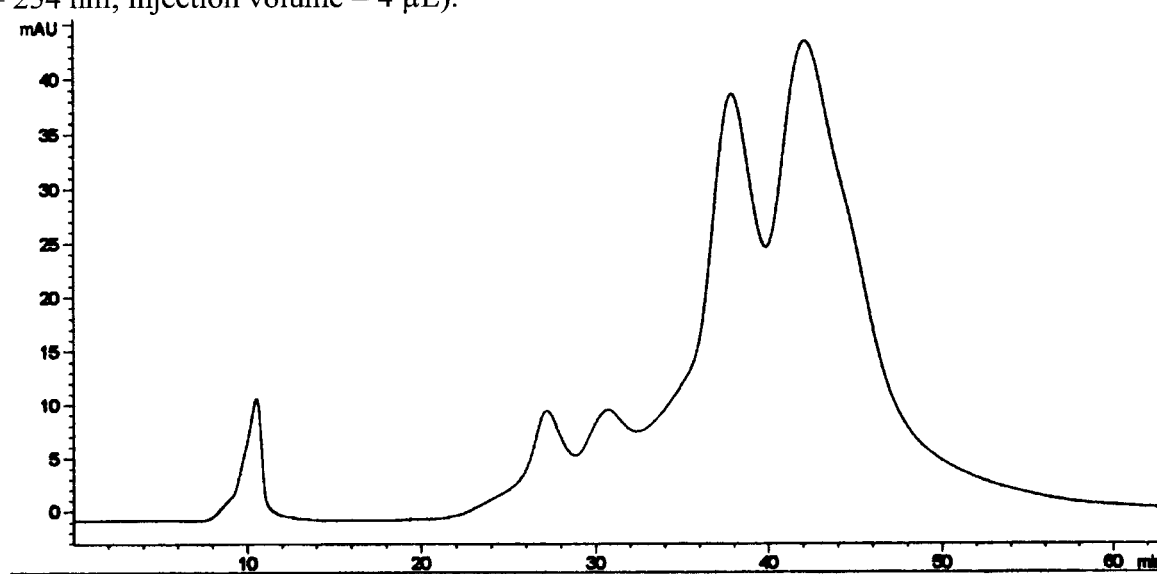
Figure 49. Separation of enantiomers of SW-II-69B (substituted β-cyclodextrin column; mobile phase - 60% methanol:40% water; flow rate = 0.5 mL/min; temperature = 25°C; λ = 254 nm; injection volume = 4 μL).

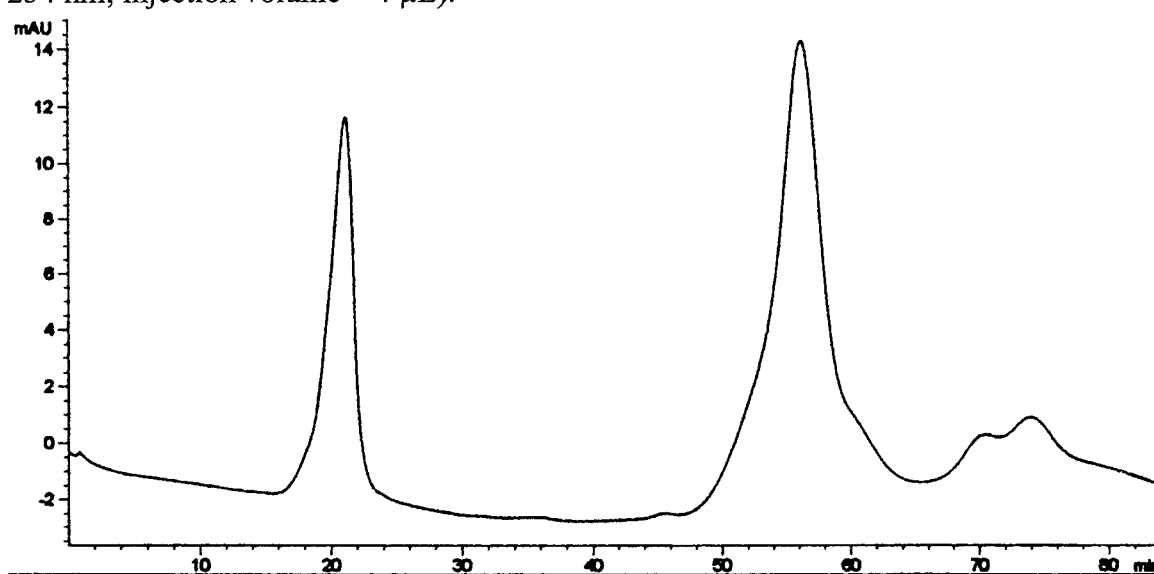Figure 50. Separation of enantiomers of SW-II-69B (substituted β-cyclodextrin column; mobile phase - 40% acetonitrile:60% water; flow rate = 0.5 mL/min; temperature = 25°C; λ = 254 nm; injection volume = 20 μL).
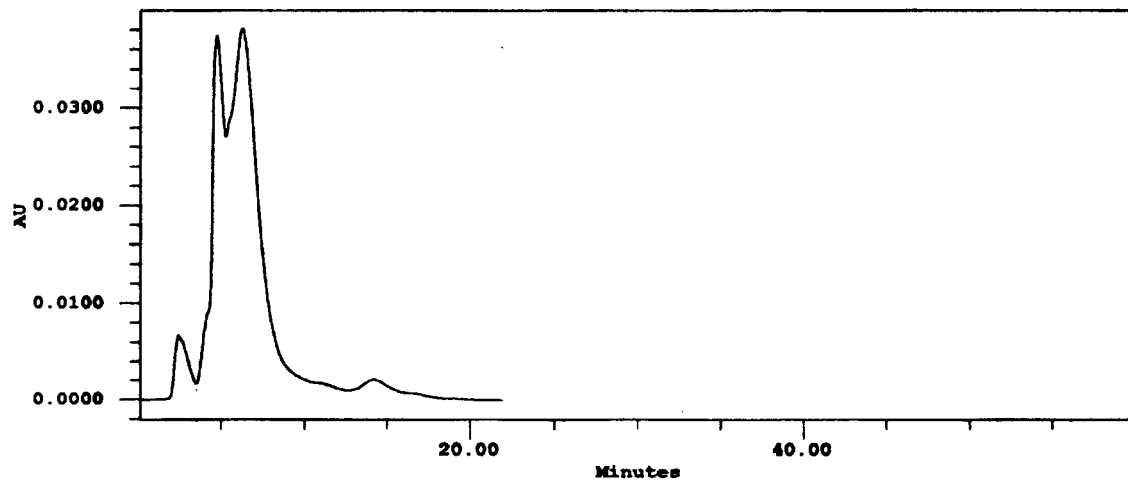

112

Table 29. Mobile phase composition and retention times for the substituted beta-cyclodextrin column using SW-II-71B as the solute.

mobile phase composition	tr (min)	k'	alpha
70% methanol	32.82	15.41	
	34.99	16.50	1.07
60% methanol	21.25	9.63	
	59.36	28.68	2.98
50% methanol	19.50	11.19	
	24.25	14.16	1.27
80% acetonitrile	3.07	0.53	
	3.10	0.55	1.03
40% acetonitrile	5.37	1.68	
	6.34	2.17	1.29

Table 30. Mobile phase composition and retention times for the quinine column using SW-II-71B as the solute.

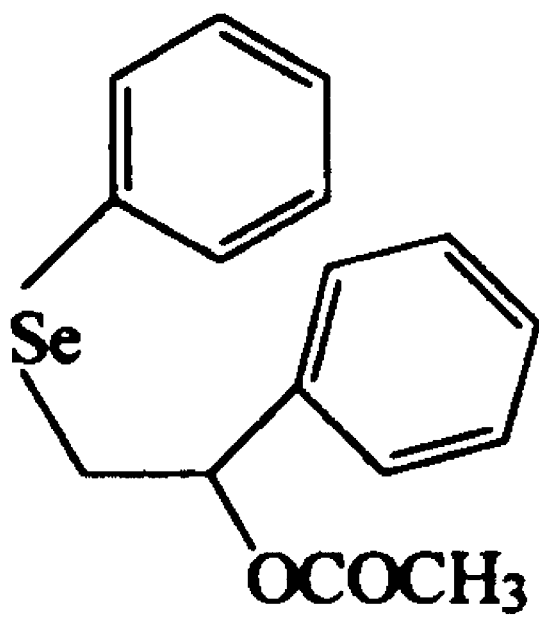| mobile phase composition	tr (min)	k'	alpha
80% methanol	4.08	1.04	
	4.38	1.19	1.14

Figure 51. Structure of SW-II-71B.

Figure 52. Separation of enantiomers of SW-II-71B (substituted β-cyclodextrin column; mobile phase - 70% methanol:30% water; flow rate = 0.5 mL/min; temperature = 25°C; λ = 254 nm; injection volume = 4 μL).
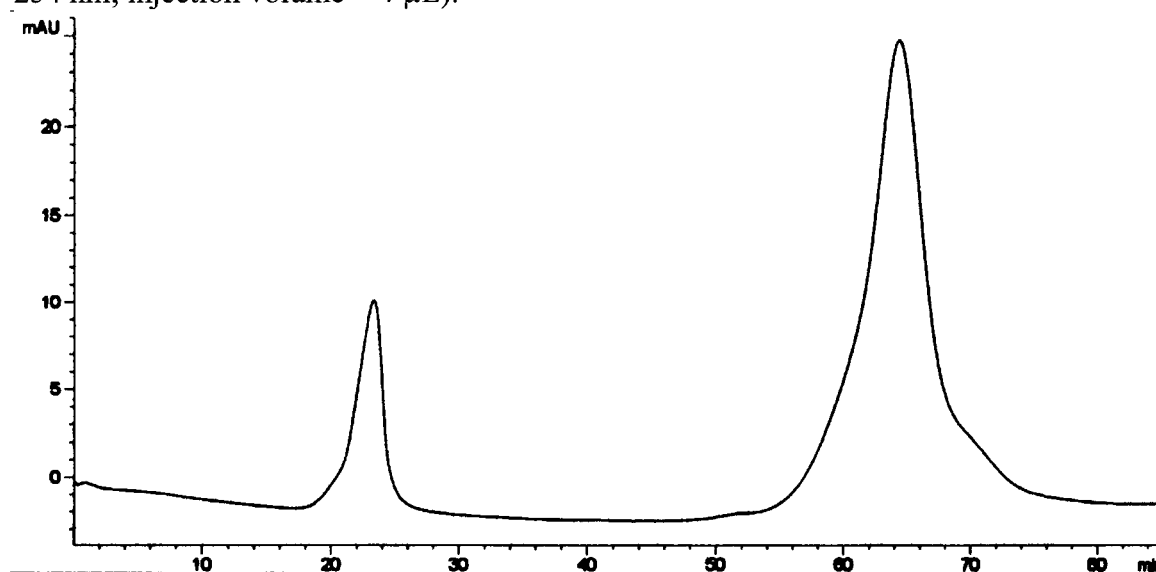
Table 31. Mobile phase composition and retention times for the substituted beta-cyclodextrin column using SW-II-73B-OH as the solute.

mobile phase composition	tr (min)	k'	alpha
70% methanol	39.17	18.59	
	43.96	20.98	1.13
40% acetonitrile	3.17	0.58	
	3.38	0.69	1.18

Table 32. Mobile phase composition and retention times for the quinine column using SW-II-73B-OH as the solute.

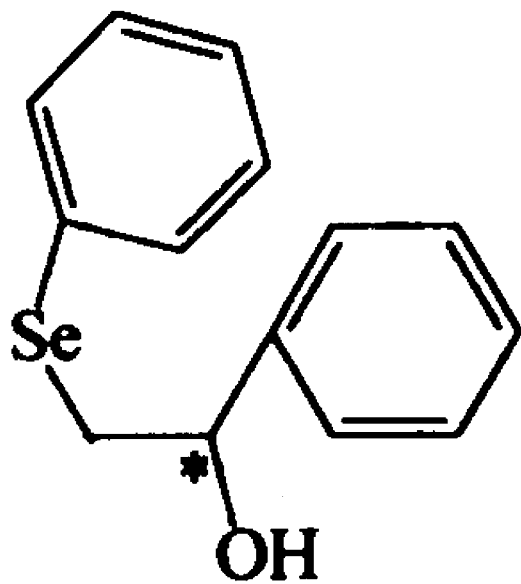| mobile phase composition	tr (min)	k'	alpha
80% methanol	4.12	1.06	
	4.32	1.16	1.09

Figure 53. Structure of SW-II-73B-OH.

Figure 54. Separation of enantiomers of SW-II-73B-OH (substituted β-cyclodextrin column; mobile phase - 70% methanol:30% water; flow rate = 0.5 mL/min; temperature = 25°C; λ = 254 nm; injection volume = 4 μL).
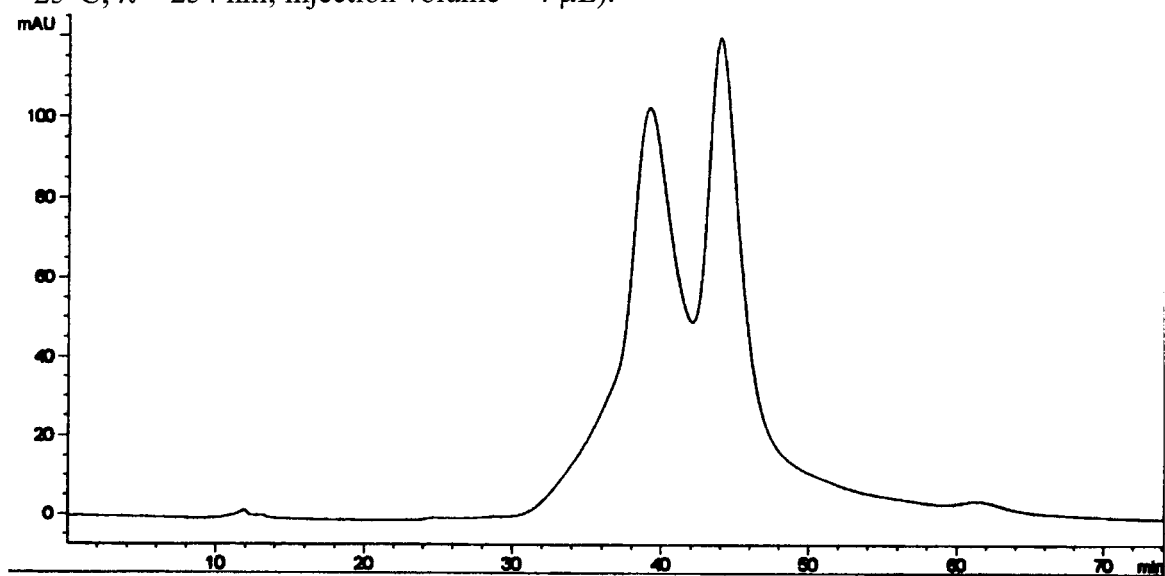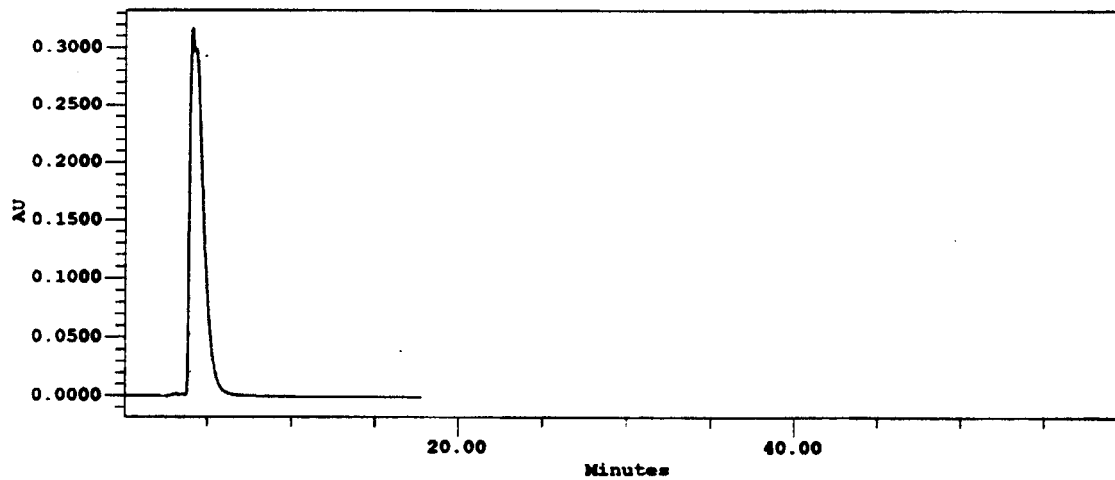
Figure 55. Separation of enantiomers of SW-II-73B-OH (substituted quinine column; mobile phase - 80% methanol:20% water; flow rate = 0.5 mL/min; temperature = 25°C; λ = 254 nm; injection volume = 20 μL).

enantiomers of SW-II-81A than the quinine column. Tables 37-38 show that the solutes were retained longer and its enantiomers were resolved better on the cyclodextrin column. Figure 63 shows the structure of SW-II-81A. Due to the presence of 1 chiral center and 2 rings, Pirkle type interactions result in enantiomeric separation on the quinine column. The lone ring structure favor separation on the cyclodextrin CSP. Figures 64-66 are chromatograms showing successful separations.

The substituted β-cyclodextrin column was more successful in separating the enantiomers of SW-II-83B than the quinine column. Tables 39-40 show that the quinine had better peak resolving ability as evident by the alpha value of 1.50. Figure 67 shows the structure of SW-II-83B. Due to the presence of 1 chiral center, 1 ring, and 1 hydroxyl group, Pirkle type interactions result in enantiomeric separation on the quinine column, while the aromatic ring favor inclusion complex formation.

G. pH Effects on the Quinine Column

Two different solvent systems were used: 0.05 M potassium phosphate (pH 2.0) and 0.1 M KH_2PO_4 (pH 7.0). Both solvent systems were used to examine and explore buffer pH effects on the quinine column's separation abilities. There was no separation observed for the three solutes tested: nortriptyline, 2-phenyl-1,2-propanediol, and SW-II-75B-OCH$_3$. Somehow, the pH of the solvent systems interfered with the chiral separation process. The components of the mobile phases probably associate with the stationary phase or solute resulting in the destruction of chiral recognition. This study consisted of a few preliminary test or exploration on pH effects. Consequently, more

Table 33. Mobile phase composition and retention times for the substituted beta-cyclodextrin column using SW-II-75B-OCH$_3$ as the solute.

mobile phase composition	tr (min)	k'	alpha
70% methanol	35.12	16.56	
	40.73	19.36	1.22
60% methanol	13.09	7.18	
	15.49	8.68	1.21
50% methanol	26.00	15.25	
	31.49	18.68	1.23
80% acetonitrile	3.19	0.60	
	3.84	0.92	1.54
60% acetonitrile	3.26	0.63	
	3.49	0.75	1.19

Table 34. Mobile phase composition and retention times for the quinine column using SW-II-75B-OCH$_3$ as the solute.

mobile phase composition	tr (min)	k'	alpha
80% methanol	4.13	1.07	
	4.33	1.16	1.09

121

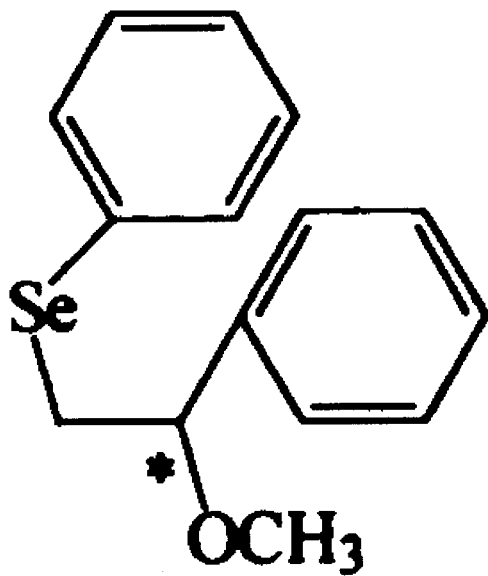Figure 56. Structure of SW-II-75B-OCH3.

Figure 57. Separation of enantiomers of SW-II-75B-OCH$_3$ (substituted β-cyclodextrin column; mobile phase - 70% methanol:30% water; flow rate = 0.5 mL/min; temperature = 25°C; λ = 254 nm; injection volume = 4 μL).
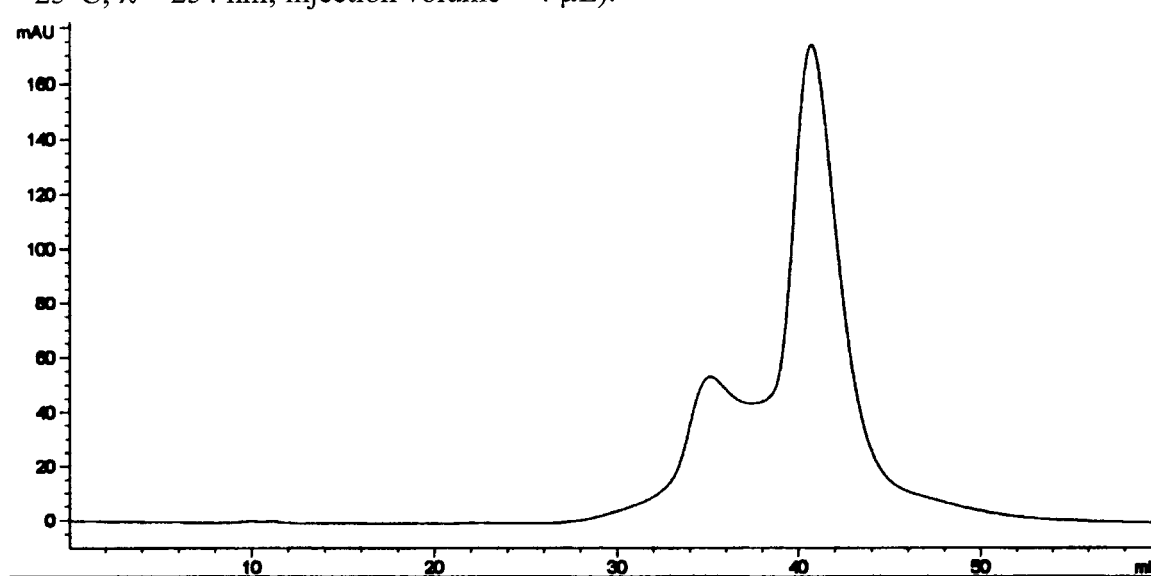
Figure 58. Separation of enantiomers of SW-II-75B-OCH₃ (substituted β-cyclodextrin column; mobile phase - 60% methanol:40% water; flow rate = 0.4 mL/min; temperature = 25°C; λ = 254 nm; injection volume = 4 µL).
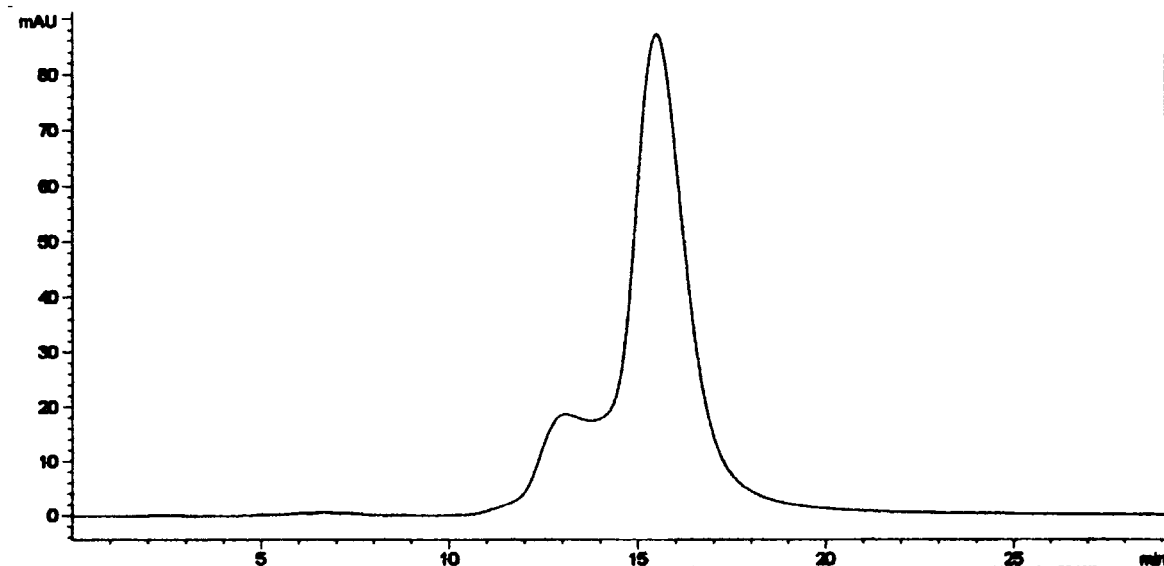
Figure 59. Separation of enantiomers of SW-II-75B-OCH₃ (substituted quinine column; mobile phase - 80% methanol:20% water; flow rate = 0.5 mL/min; temperature = 25°C; λ = 254 nm; injection volume = 20 μL).
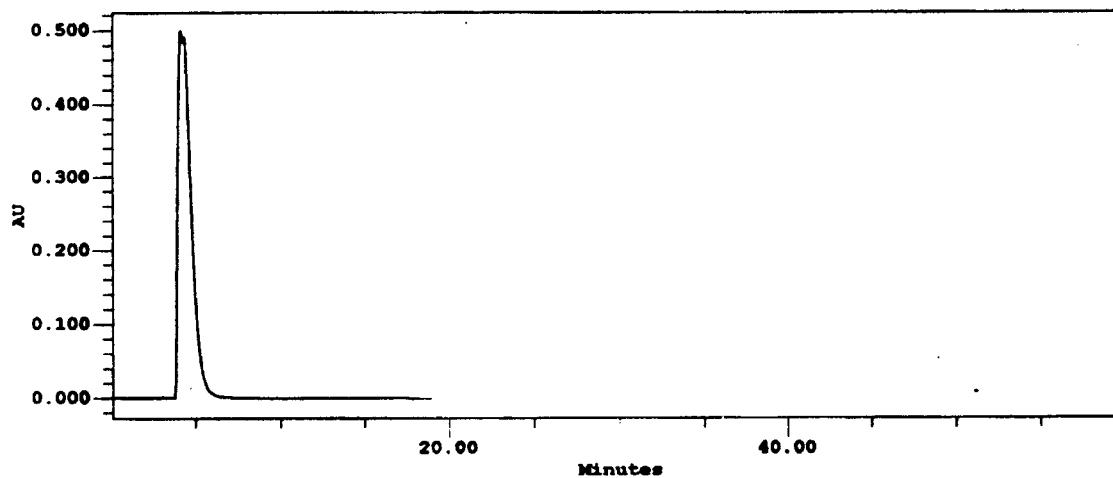
Table 35. Mobile phase composition and retention times for the substituted beta-cyclodextrin column using SW-II-79B as the solute.

mobile phase composition	tr (min)	k'	alpha
70% methanol	29.30	13.65	
	33.83	15.92	1.17
60% methanol	7.73	3.83	
	9.35	4.84	1.27
50% methanol	9.71	5.07	
	11.91	6.45	1.27
80% acetonitrile	3.24	0.62	
	3.40	0.70	1.13
40% acetonitrile	4.87	1.44	
	6.74	2.37	1.65

Table 36. Mobile phase composition and retention times for the quinine column using SW-II-79B as the solute.

mobile phase composition	tr (min)	k'	alpha
80% methanol	4.15	1.07	
	4.33	1.17	1.08
60% acetonitrile	4.40	1.20	
	4.49	1.25	1.04

126

Figure 60. Structure of SW-II-79B.

Figure 61. Separation of enantiomers of SW-II-79B (substituted β-cyclodextrin column; mobile phase - 70% methanol:30% water; flow rate = 0.5 mL/min; temperature = 25°C; λ = 254 nm; injection volume = 4 μL).
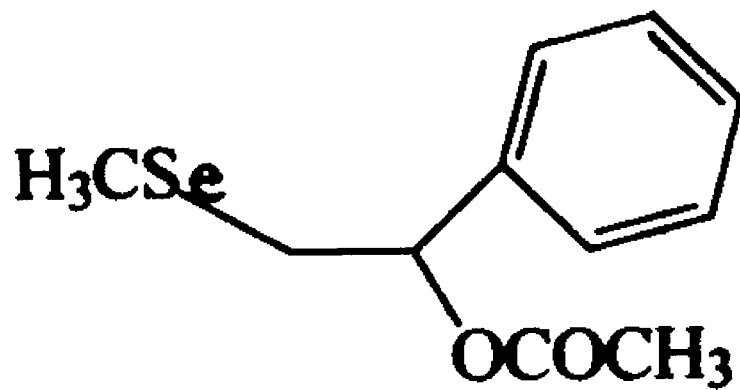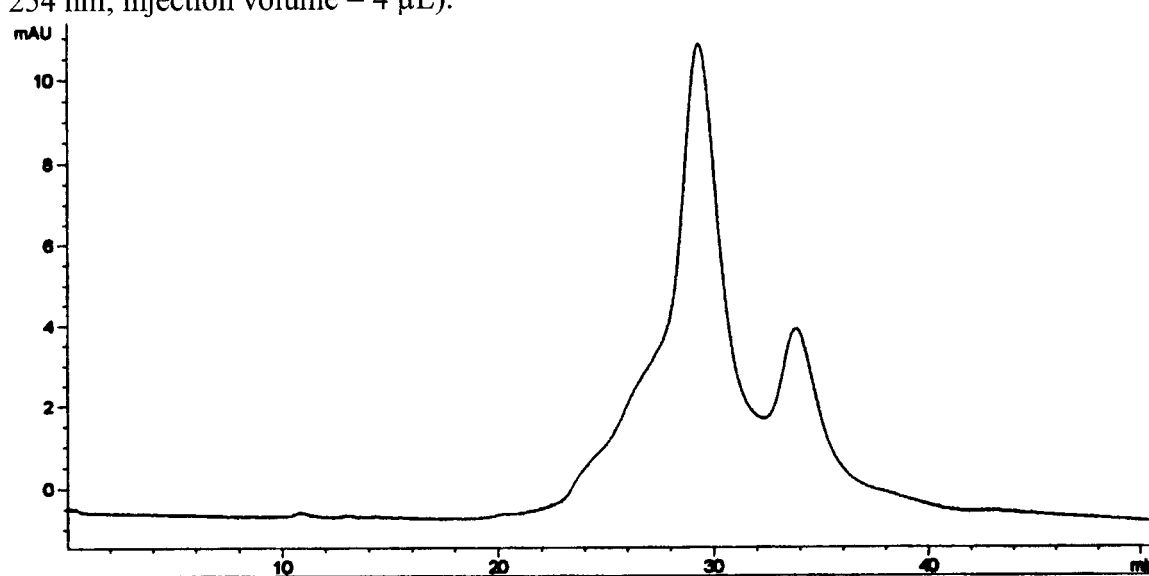
Figure 62. Separation of enantiomers of SW-II-79B (substituted β-cyclodextrin column; mobile phase - 60% methanol:40% water; flow rate = 0.4 mL/min; temperature = 25°C; λ = 254 nm; injection volume = 4 μL).
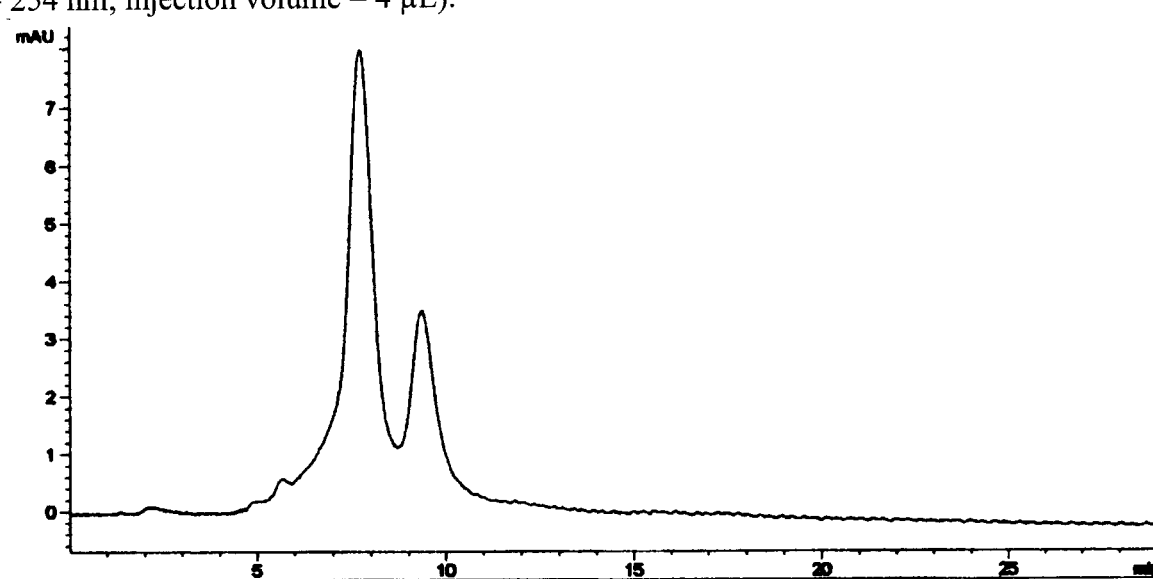
Table 37. Mobile phase composition and retention times for the substituted beta-cyclodextrin column using SW-II-81A as the solute.

mobile phase composition	tr (min)	k'	alpha
70% methanol	35.20	16.60	
	38.00	18.00	1.08
60% methanol	11.16	5.97	
	12.14	6.59	1.10
40% acetonitrile	4.70	1.35	
	5.66	1.83	1.36

Table 38. Mobile phase composition and retention times for the quinine column using SW-II-81A as the solute.

mobile phase composition	tr (min)	k'	alpha
80% methanol	4.15	1.08	
	4.32	1.16	1.08

Figure 63. Structure of SW-II-81A.

Figure 64. Separation of enantiomers of SW-II-81A (substituted β-cyclodextrin column; mobile phase - 70% methanol:30% water; flow rate = 0.5 mL/min; temperature = 25°C; λ = 254 nm; injection volume = 4 μL).
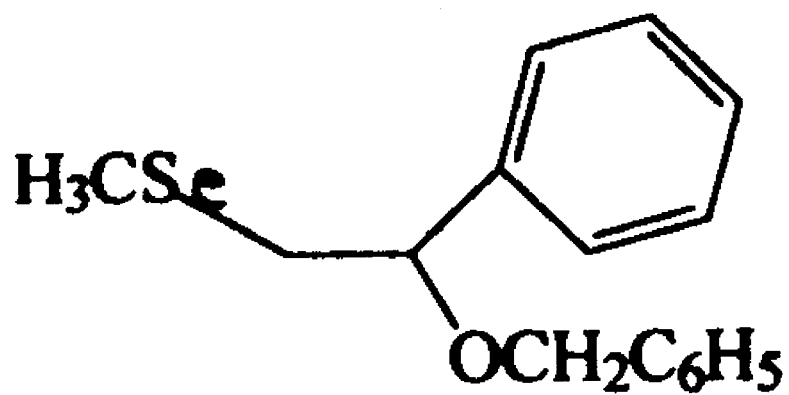
Figure 65. Separation of enantiomers of SW-II-81A (substituted β-cyclodextrin column; mobile phase - 60% methanol:40% water; flow rate = 0.4 mL/min; temperature = 25°C; λ = 254 nm; injection volume = 4 μL).
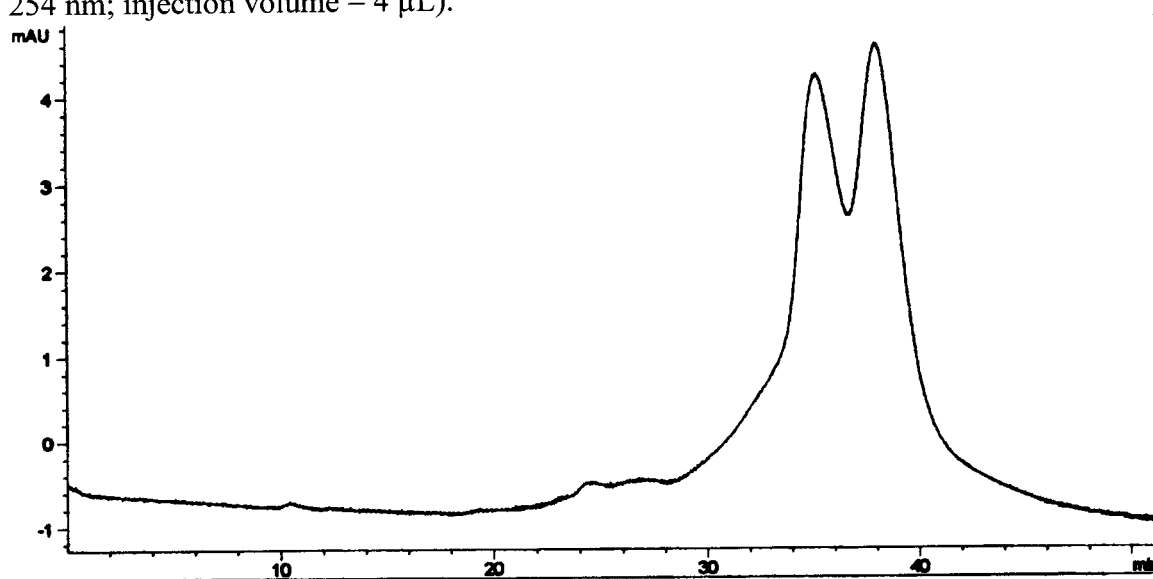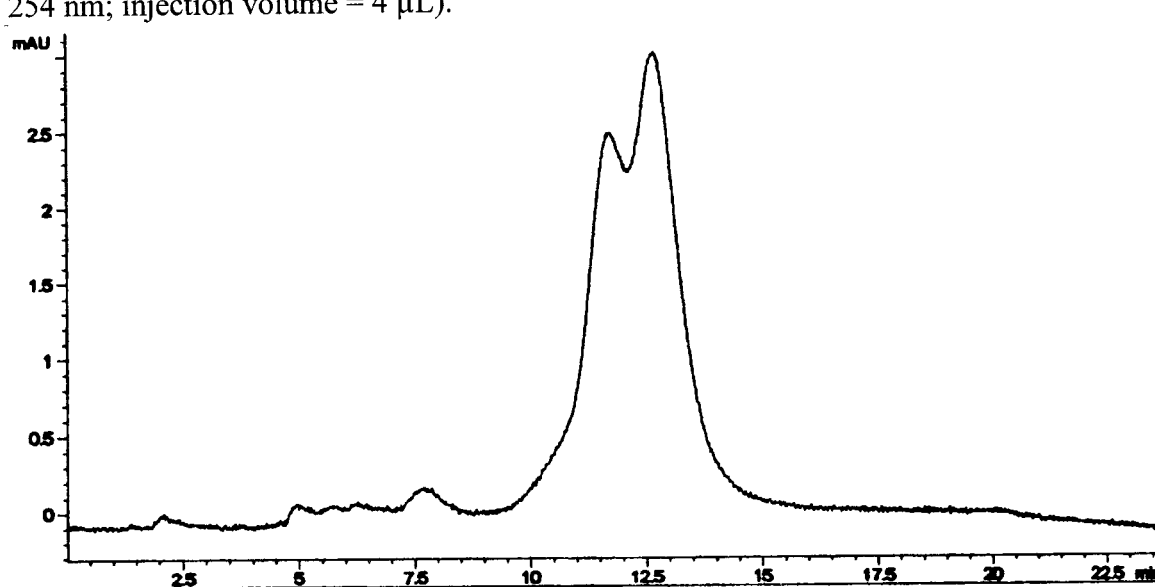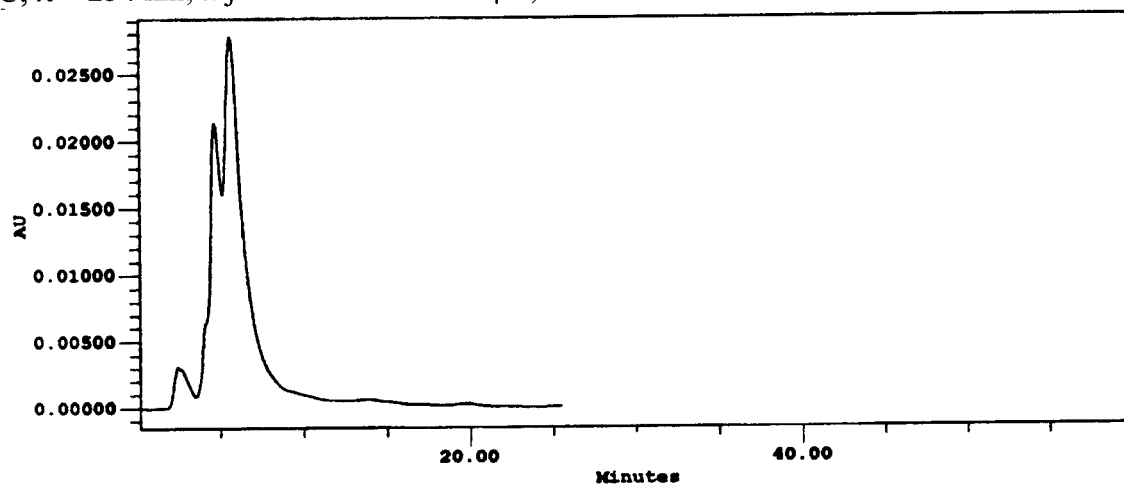
Figure 66. Separation of enantiomers of SW-II-81A (substituted β-cyclodextrin column; mobile phase - 40% acetonitrile:60% water; flow rate = 0.5 mL/min; temperature = 25°C; λ = 254 nm; injection volume = 20 μL).

134

extensive testing of various CSPs, solutes, buffers, and pH conditions must be done to

have a conclusive knowledge of pH effects on chiral separation.

Table 39. Mobile phase composition and retention times for the substituted
beta-cyclodextrin column using SW-II-83B as the solute.

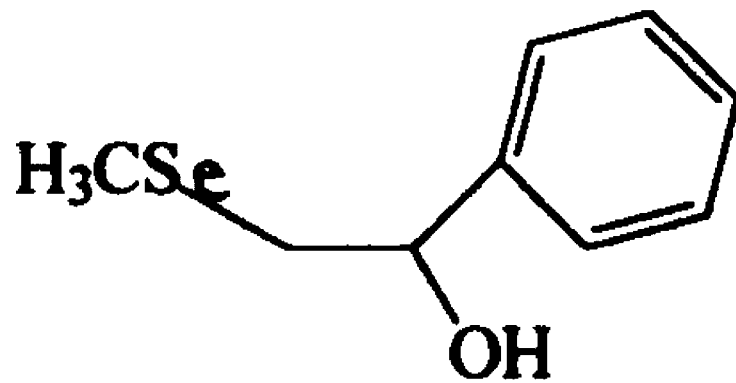| mobile phase composition	tr (min)	k'	alpha
90% acetonitrile	3.28	0.64	
	3.61	0.81	1.26
60% acetonitrile	3.56	0.78	
	3.62	0.81	1.04
40% acetonitrile	4.74	1.37	
	5.08	1.54	1.13

Table 40. Mobile phase composition and retention times for the quinine
column using SW-II-83B as the solute.

mobile phase composition	tr (min)	k'	alpha
40% methanol	4.50	1.25	
	5.75	1.88	1.50

Figure 67. Structure of SW-II-83B.

CHAPTER IV

CONCLUSIONS

TES silanization/hydrosilation is an effective reaction method to synthesize chiral

stationary phases. Organic groups with a terminal olefin, such as quinine, can be directly

attached to silica to form hydrophobic surfaces. Successful bonding of the organic group

to the silica surface can be determined by DRIFT spectroscopy, ^{13}C CP-MAS NMR

spectroscopy, and elemental analysis.

Using two solvent systems (methanol:water and acetonitrile:water), both the 2-

hydroxy-3-methacryloyloxypropyl-β-cyclodextrin column and quinine column were able

to separate various solutes. Enantiomers of binaphthol, TFAE, various antibiotics,

various drugs, homatropine, 2-phenoxypropionic acid, various alcohols, $[Ru(bipy)_3]^{2+}$,

and novel Selenium compounds were resolved. The 2-hydroxy-3-

methacryloyloxypropyl-β-cyclodextrin column had more success in separation than the

quinine column likely due to the substituted β-cyclodextrin's myriad array of potential

interactions: electrostatic interactions, hydrogen bonding, dipole stacking, hydrophobic

interactions, steric repulsions, and formation of inclusion complexes. Overall, the

substituted beta-cyclodextrin column had a total of 55 successful separations in

comparison to 27 successful separations by the quinine column. Each type of CSP had

different successes based on the type of solute. For instance, the antibiotics'

(chlortetracycline and tetracycline) enantiomers were separated better on the quinine

column. In contrast, drugs (e.g. tropicamide), alcohols (e.g. DL-propranolol), and novel

Selenium compounds (e.g. SW-II-69B) were separated better on the cyclodextrin column.

One explanation why Selenium compounds were resolved better on the cyclodextrin

column is a combination of chirality, hydrophobicity from the rings, and size that

conforms to the hydrophobic cavity of the substituted beta-cyclodextrin. Quinine's

ability to separate solutes was impaired by using buffers at pH 2.0 and 7.0.

REFERENCES

1. Boyer, R.; <u>Modern Experimental Biochemistry</u>, Benjamin Cummings, **2000**, Chapter 3.

2. Yu, X.; Zhao, R.; Liu, G. Q.; *Chromatographia* **2000**, 52(7/8), 517-519.

3. Vollhardt, K. P. C.; Schore, N. E.; <u>Organic Chemistry</u>, W. H. Freeman and Company, **1994**, Chapter 5.

4. Stinson, S. C.; *C&EN* **2000**, 55-78.

5. Carey, F. A.; Sundberg, R. J.; <u>Advanced Organic Chemistry</u>, Kluwer Academic/Plenum Publishers, **2000**, Chapter 2.

6. Alvarez, C.; Sanchez-Brunete, J. A.; Torrado-Santiago, S.; Cadorniga, R.; Torrado, J. J.; *Chromatographia* **2000**, 52(7/8), 455-458.

7. De Camp, W.; *Chirality* **1989**, 1(1), 2-6.

8. Pesek, J. J.; Matyska, M. T.; Fu, P. F.; *Chromatographia* **2001**, 53, 635-640.

9. Pesek, J. J.; Matyska, M. T.; Sandoval, J. E.; Williamsen, E. J.; *J. Liq. Chrom. & Rel. Technol.* **1996**, 19(17&18), 2843-2865.

10. Stuurman, H. W.; Kohler, J.; Schomburg, G.; *Chromatographia* **1988**, 25(4), 265-271.

11. Tertykh, V. A.; Yanishpolskii, V. V.; Bereza, L. V.; Pesek, J. J. Matyska, M.; *Journal of Thermal Analysis and Calorimetry* **2000**, 62, 539-544.

12. Pesek, J. J.; Matyska, M. T.; Williamsen, E. J.; Evanchic, M.; Hazari, V.; Konjuh, K.; Takhar, S.; Tranchina, R.; *J. Chromatogr. A.* **1997**, 786, 219-228.

13. Pesek, J. J.; Matyska, M. T.; Muley, S.; *Chromatographia* **2000**, 52, 439-444.

14. Pesek, J. J.; Matyska, M. T.; Menezes, S.; *J. Chromatogr. A.* **1999**, 853, 151-158.

15. Pesek, J. J.; Matyska, M. T.; Cho, S.; *J. Chromatogr. A.* **1999**, 845, 237-246.

16. Skoog, D. A.; Holler, F. J.; Nieman, T. A.; <u>Principles of Instrumental Analysis</u>, Saunders College Publishing, **1998**, Chapters 7, 17, 19, and 33.